The AeroCom evaluation and intercomparison of organic aerosol in global models

K. Tsigaridis[1,2,*], N. Daskalakis[3,4], M. Kanakidou[3,*], P. J. Adams[5,6], P. Artaxo[7], R. Bahadur[8], Y. Balkanski[9], S. E. Bauer[1,2], N. Bellouin[10,11], A. Benedetti[12], T. Bergman[13], T. K. Berntsen[14,15], J. P. Beukes[16], H. Bian[17], K. S. Carslaw[18], M. Chin[19], G. Curci[20], T. Diehl[19,21], R. C. Easter[22], S. J. Ghan[22], S. L. Gong[23], A. Hodzic[24], C. R. Hoyle[25], T. Iversen[12,26,14], S. Jathar[5], J. L. Jimenez[27], J. W. Kaiser[28,12,29], A. Kirkevåg[26], D. Koch[1,2,30], H. Kokkola[13], Y. H. Lee[5,31], G. Lin[32], X. Liu[22], G. Luo[33], X. Ma[34,35], G. W. Mann[36,37], N. Mihalopoulos[3], J.-J. Morcrette[12], J.-F. Müller[38], G. Myhre[15], S. Myriokefalitakis[3,4], S. Ng[39], D. O'Donnell[40,41], J. E. Penner[32], L. Pozzoli[42], K. J. Pringle[43,29], L. M. Russell[8], M. Schulz[26], J. Sciare[9], Ø. Seland[26], D. T. Shindell[2,1], S. Sillman[32], R. B. Skeie[15], D. Spracklen[18], T. Stavrakou[38], S. D. Steenrod[21], T. Takemura[44], P. Tiitta[16,45], S. Tilmes[24], H. Tost[46], T. van Noije[47], P. G. van Zyl[16], K. von Salzen[34], F. Yu[33], Z. Wang[48], Z. Wang[49], R. A. Zaveri[22], H. Zhang[48], K. Zhang[40,50], Q. Zhang[51], X. Zhang[49]

[1]{Center for Climate Systems Research, Columbia University, New York, NY, USA}
[2]{NASA Goddard Institute for Space Studies, New York, NY, USA}
[3]{Environmental Chemical Processes Laboratory, Department of Chemistry, University of Crete, Heraklion, Greece}
[4]{Institute of Chemical Engineering, Foundation for Research and Technology Hellas (ICE-HT FORTH), Patras, Greece}
[5]{Department of Civil and Environmental Engineering, Carnegie Mellon University, Pittsburgh, PA, USA}
[6]{Department of Engineering and Public Policy, Carnegie Mellon University, Pittsburgh, PA, USA}
[7]{University of São Paulo, Brazil}
[8]{Scripps Institution of Oceanography, University of California San Diego, CA, USA}
[9]{Laboratoire des Sciences du Climat et de l'Environnement, Gif-sur-Yvette, France}
[10]{Met Office Hadley Centre, Exeter, UK}
[11]{Now at Department of Meteorology, University of Reading, Reading, UK}
[12]{ECMWF, Reading, UK}
[13]{Finnish Meteorological Institute, Kuopio, Finland}
[14]{University of Oslo, Oslo, Norway}

[15]{Center for International Climate and Environmental Research - Oslo (CICERO), Oslo, Norway}
[16]{Environmental Sciences and Management, North-West University, Potchefstroom, South Africa}
[17]{University of Maryland, Baltimore County, MD, USA}
[18]{School of Earth and Environment, University of Leeds, Leeds, UK}
[19]{NASA Goddard Space Flight Center, Greenbelt, MD, USA}
[20]{Department of Physics CETEMPS, University of L'Aquila, Italy}
[21]{Universities Space Research Association, Greenbelt, MD, USA}
[22]{Pacific Northwest National Laboratory; Richland, WA, USA}
[23]{Air Quality Research Branch, Meteorological Service of Canada, Toronto, Ontario, Canada}
[24]{National Center for Atmospheric Research, Boulder, CO, USA}
[25]{Paul Scherrer Institute, Villigen, Switzerland}
[26]{Norwegian Meteorological Institute, Oslo, Norway}
[27]{University of Colorado, Boulder, CO, USA}
[28]{King's College London, London, UK}
[29]{Department of Atmospheric Chemistry, Max Planck Institute for Chemistry, Mainz, Germany}
[30]{Now at Department of Energy, Office of Biological and Environmental Research, Washington, DC, USA}
[31]{Now at 1 and 2}
[32]{Department of Atmospheric, Oceanic, and Space Sciences, University of Michigan, Ann Arbor, MI, USA}
[33]{State University of New York, Albany, NY, USA}
[34]{Environment Canada, Victoria, Canada}
[35]{Now at 33}
[36]{National Centre for Atmospheric Science, University of Leeds, Leeds, UK}
[37]{School of Earth and Environment, University of Leeds, Leeds, UK}
[38]{Belgian Institute for Space Aeronomy, Brussels, Belgium}
[39]{Aerodyne Research, Inc., Billerica, MA, USA}
[40]{Max Planck Institute for Meteorology, Hamburg, Germany}
[41]{Now at Finnish Meteorological Institute, Helsinki, Finland}
[42]{Eurasia Institute of Earth Sciences, Istanbul Technical University, Turkey}
[43]{Institute for Climate and Atmospheric Science, School or Earth and Environment, University of Leeds, Leeds, UK}
[44]{Research Institute for Applied Mechanics, Kyushu University, Fukuoka, Japan}
[45]{Fine Particle and Aerosol Technology Laboratory, Department of Environmental Science, University of Eastern Finland, Kuopio, Finland}
[46]{Institute for Atmospheric Physics, Johannes-Gutenberg University, Mainz, Germany}
[47]{Royal Netherlands Meteorological Institute (KNMI), De Bilt, The Netherlands}
[48]{Laboratory for Climate Studies, Climate Center, China Meteorological Administration, Beijing, China}
[49]{Chinese Academy of Meteorological Sciences, Beijing, China}
[50]{Now at 22}
[51]{Department of Environmental Toxicology, University of California, Davis, CA, USA}

Correspondence to: K. Tsigaridis (kostas.tsigaridis@columbia.edu) and M. Kanakidou (mariak@chemistry.uoc.gr).

Figures

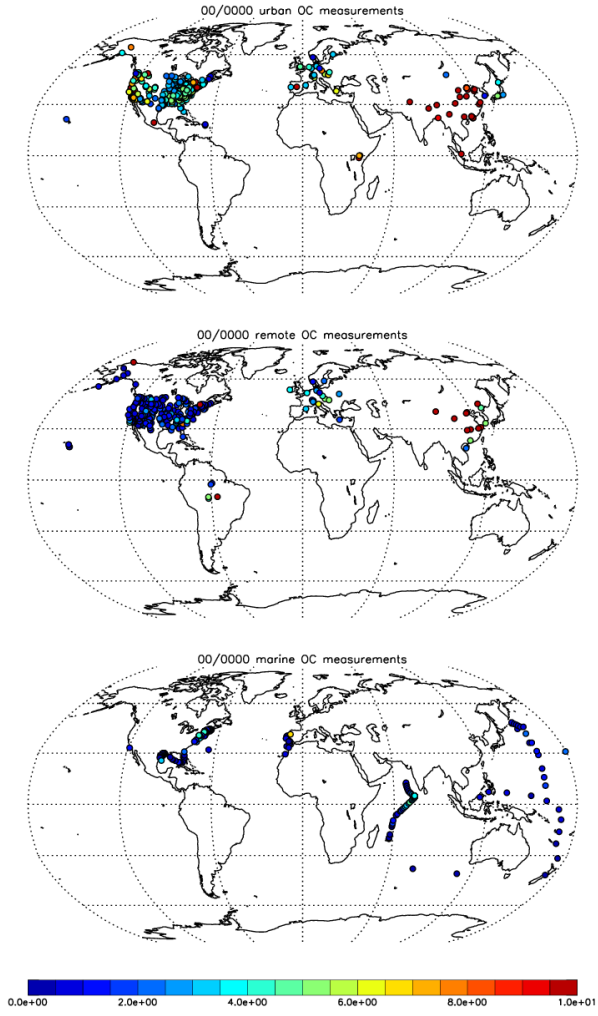

Fig. S 1. Measured OC (left) and OA (right) concentrations, for urban (top), remote (middle) and marine (bottom) locations. The date 00/0000 means all months and all years of data.

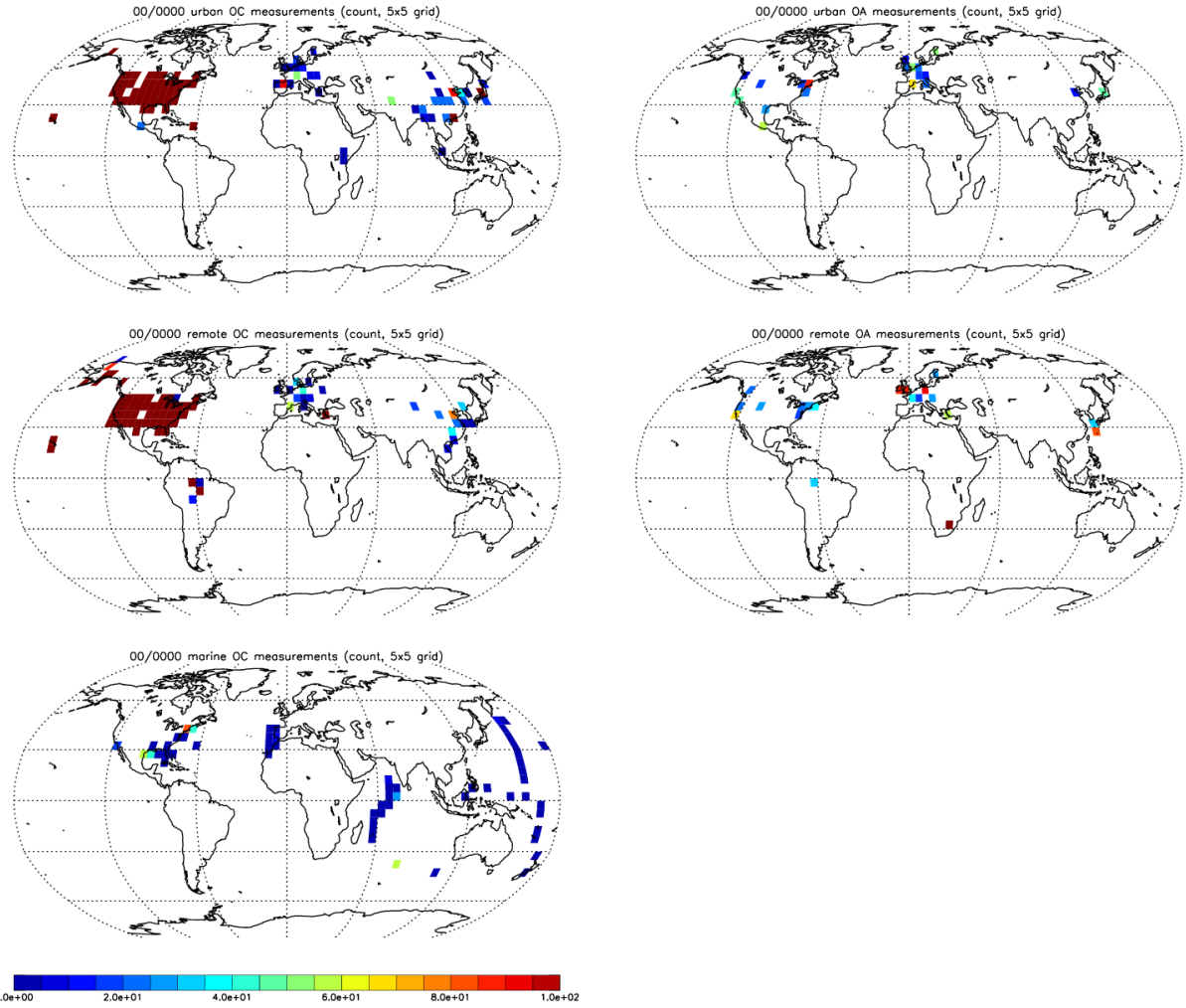

Fig. S 2. Number of data points of OC (left) and OA (right) measurements on a 5x5 grid for urban (top), remote (middle) and marine (bottom) locations. The date 00/0000 means all months and all years of data.

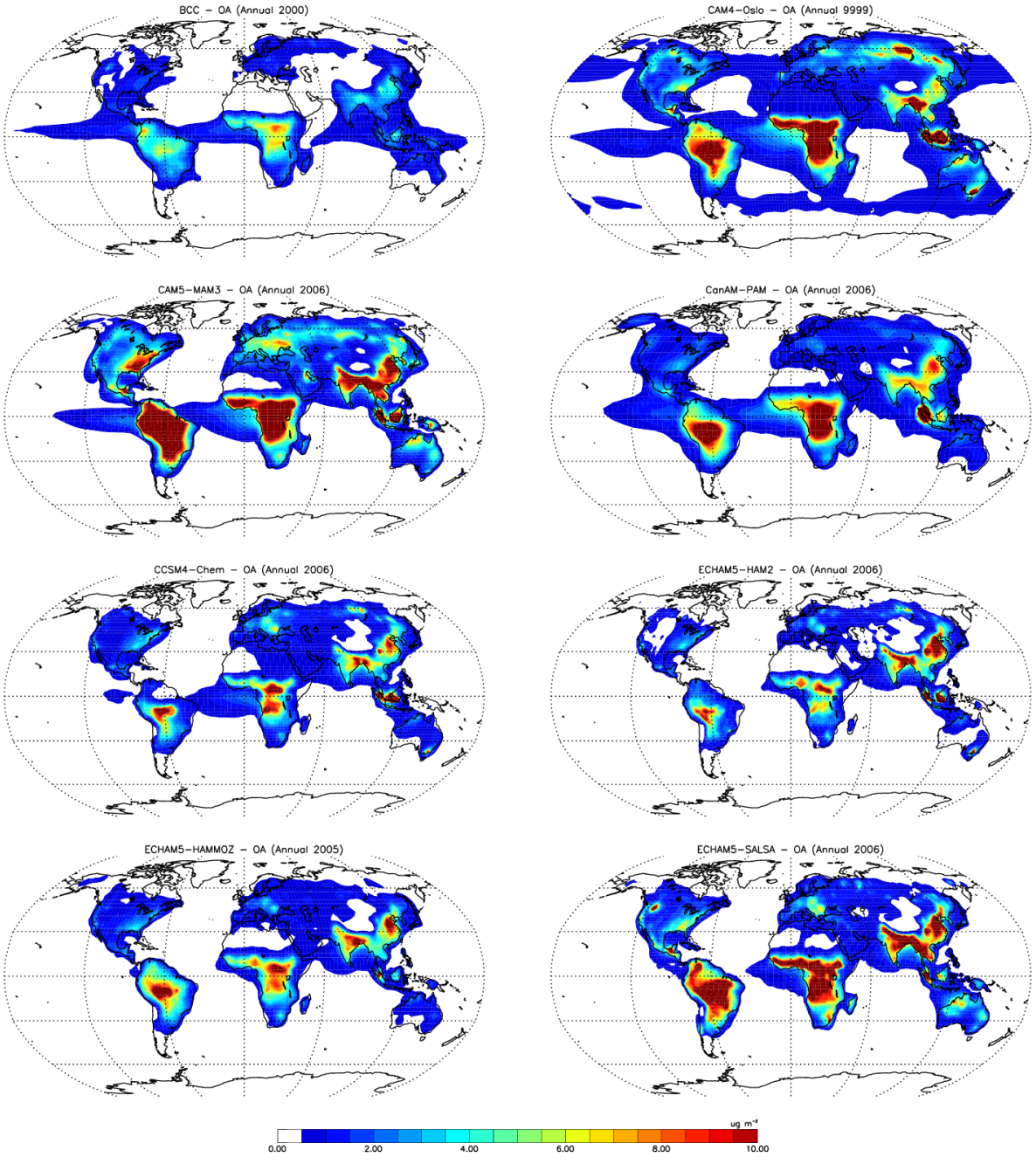

Fig. S 3. Annual mean surface OC concentration calculated by the models. The models' reference year is shown in each title; 9999 means year 2006 as defined by the emissions, but the climate was calculated online, it was not nudged to any climatology or reanalysis.

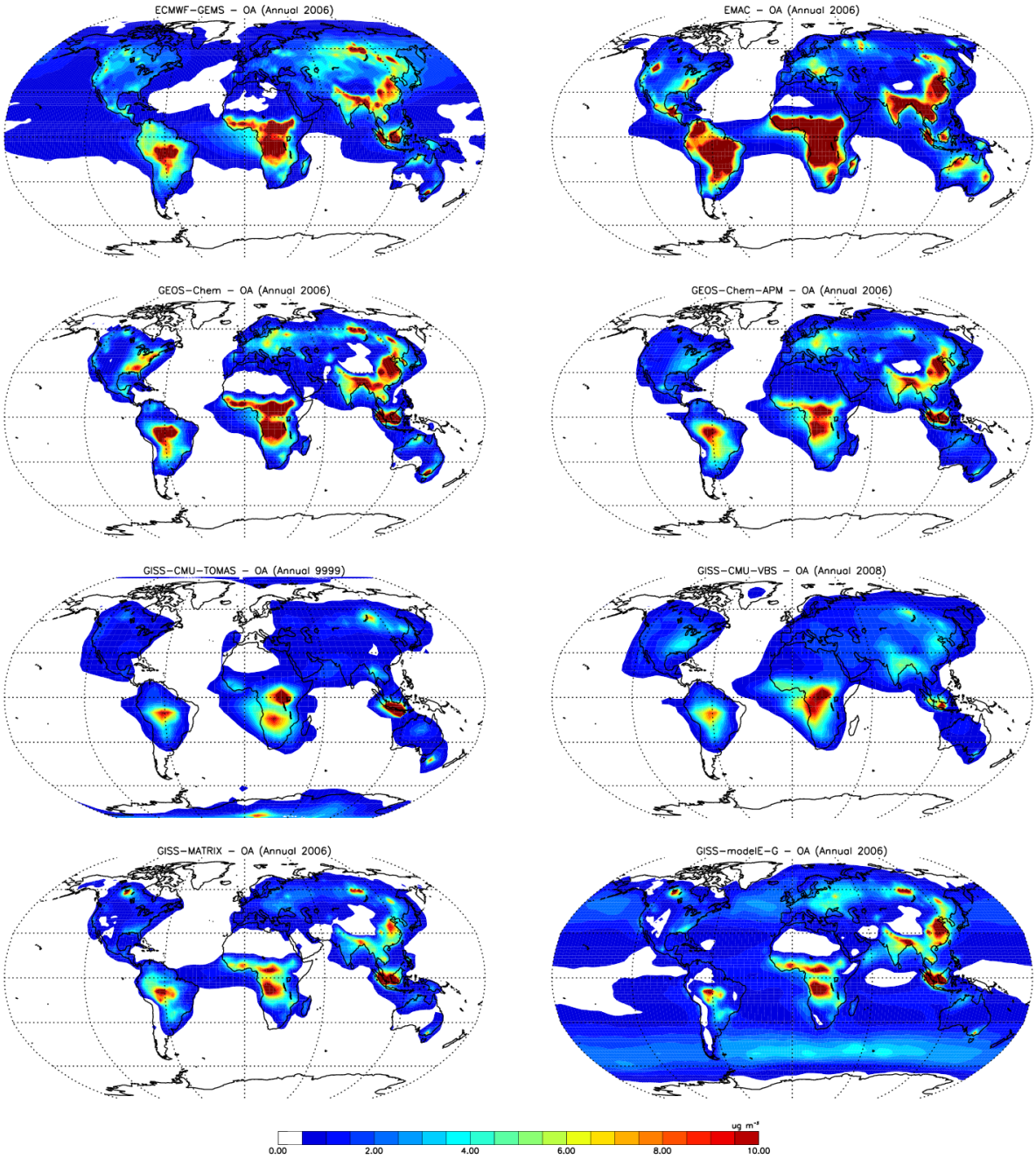

Fig. S 3, continued.

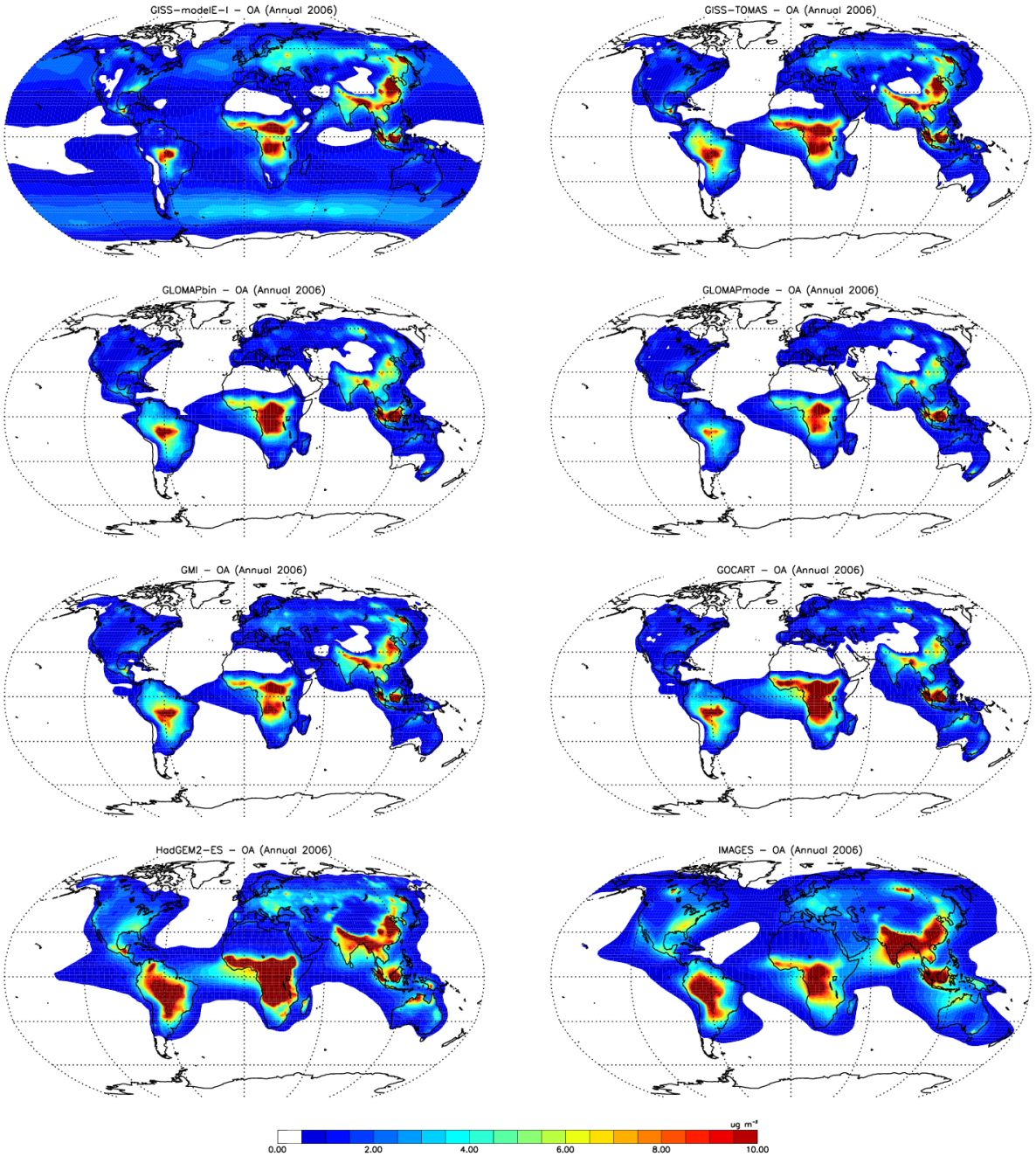

Fig. S 3, continued.

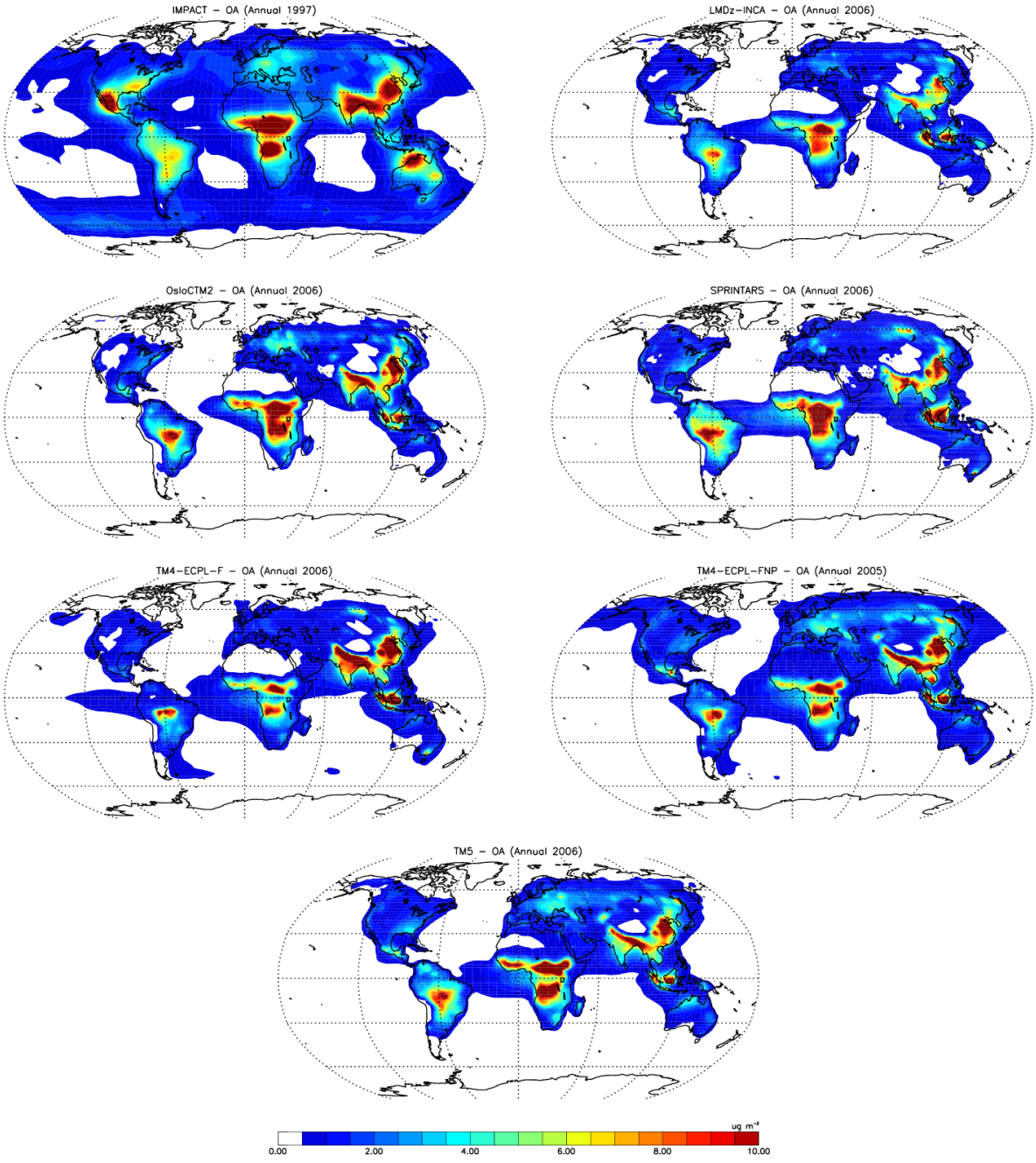

Fig. S 3, continued.

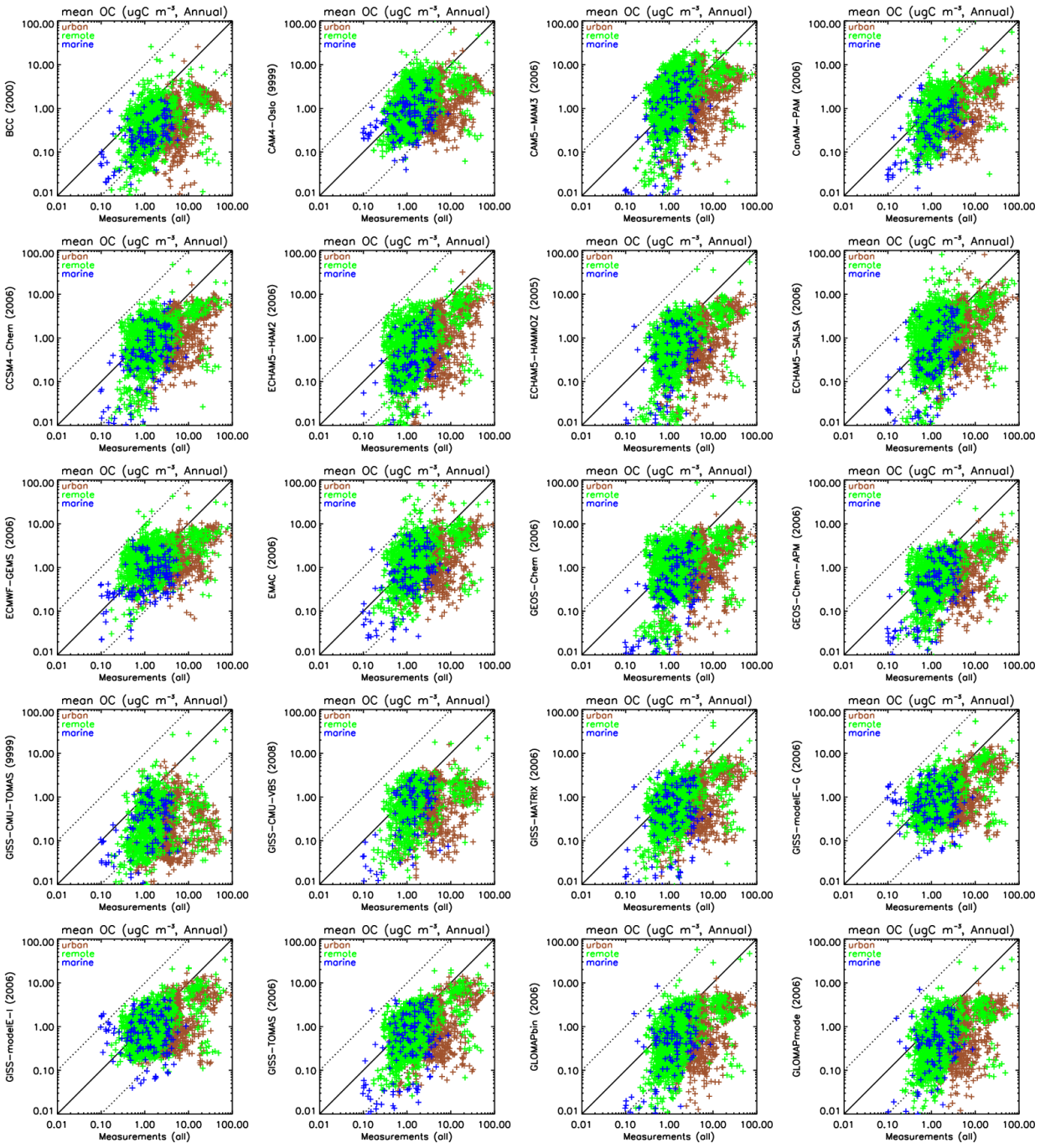

Fig. S 4. Comparison of model results with OC measurements. Stations are marked by color: urban (brown), remote (green), marine (blue). The year in parenthesis next to the model name denotes the simulated year.

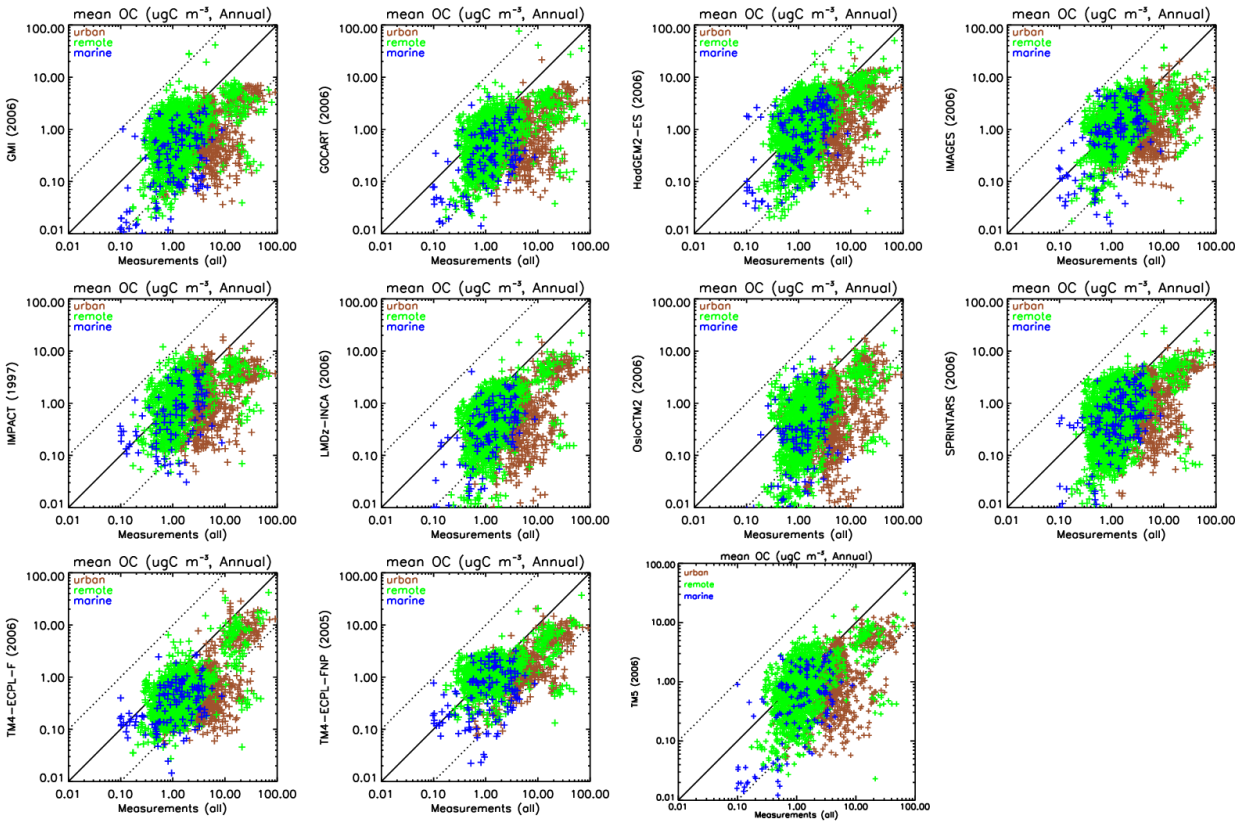

Fig. S 4, continued.

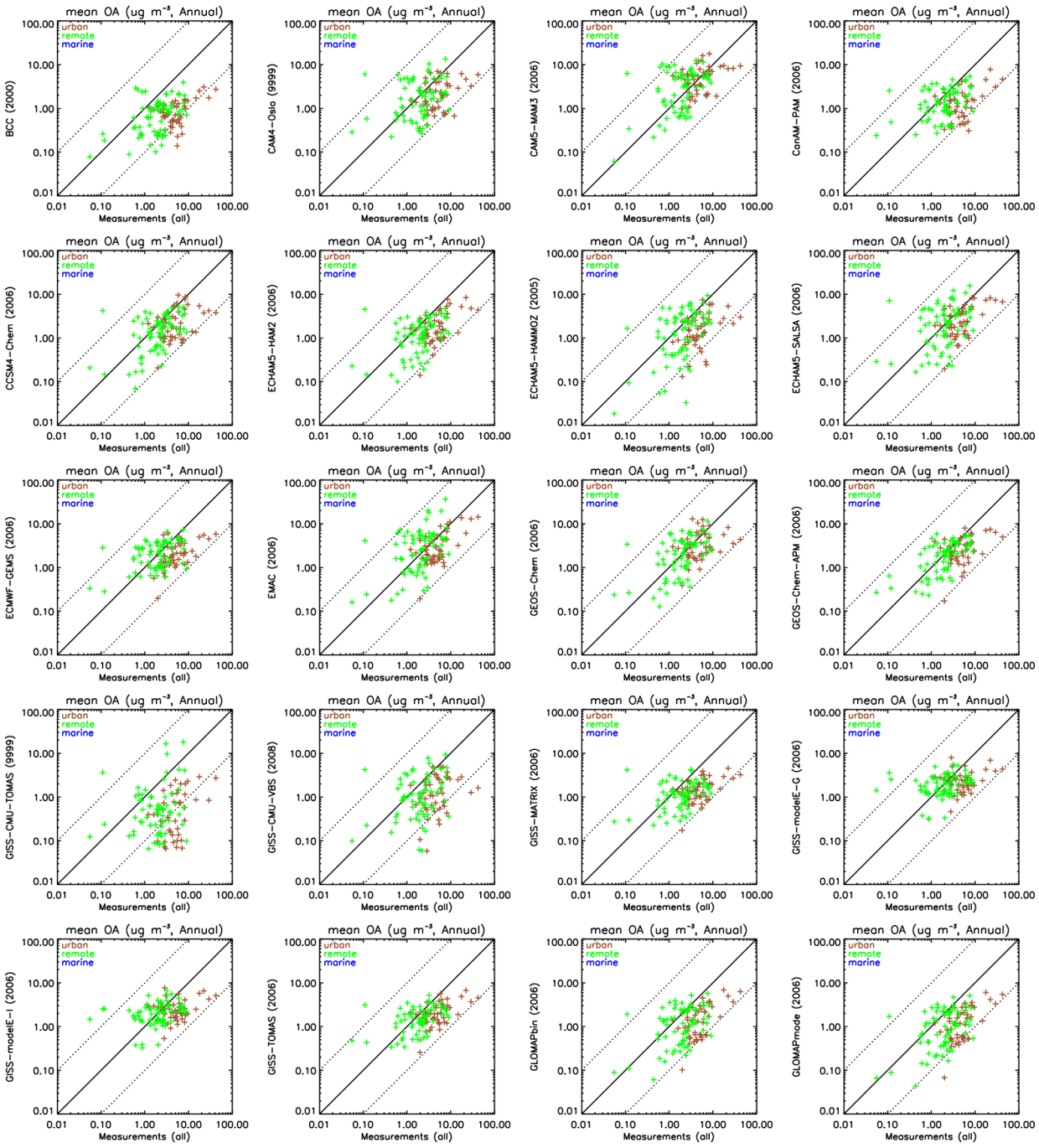

Fig. S 5. Same as Fig. S 4 for OA measurements.

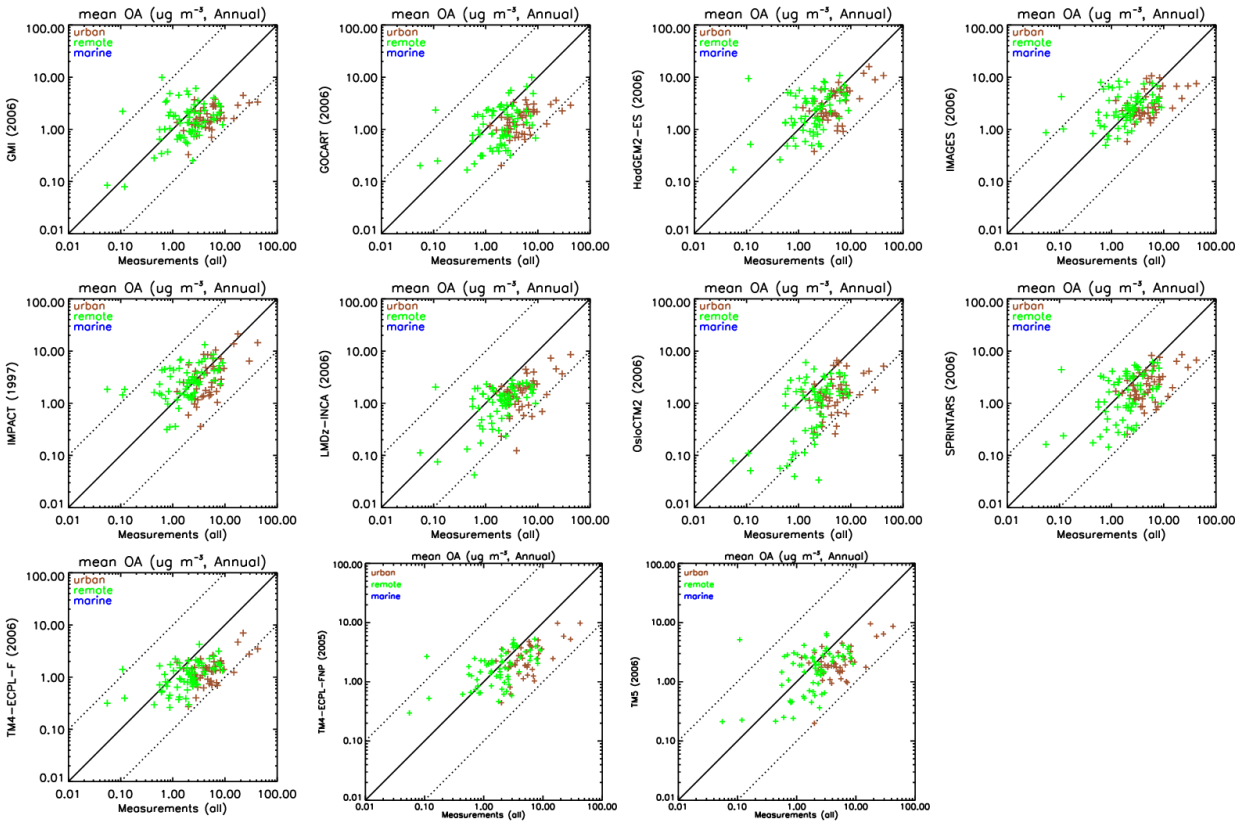

Fig. S 5, continued.

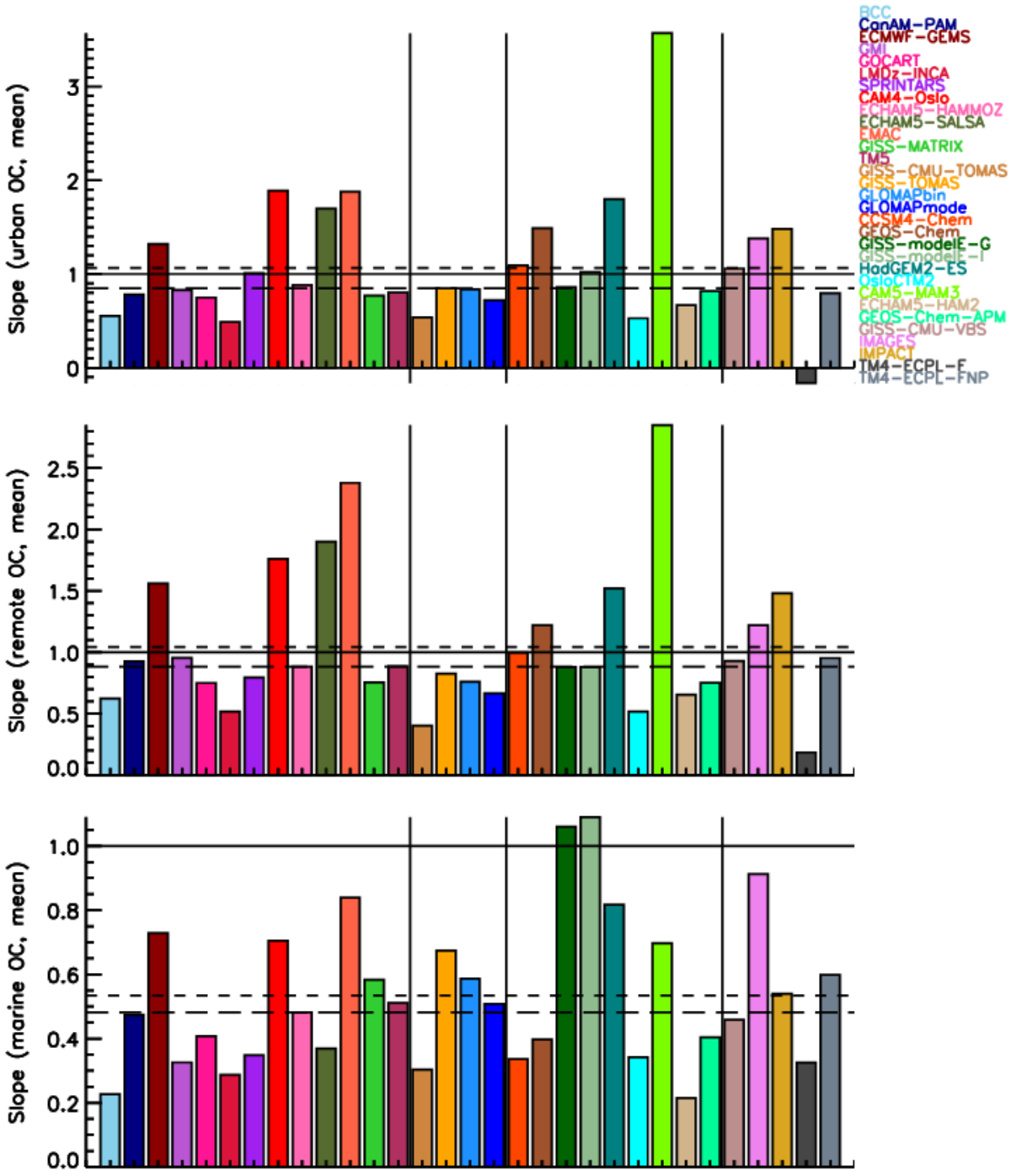

Fig. S 6. Slope of the linear regression Pearson correlation between models and OC measurements. The models are grouped based on their complexity, as separated by vertical solid lines. Groups from left to right are: SOA is directly emitted as a non-volatile tracer; SOA is chemically formed in the atmosphere but is considered non-volatile; SOA is semi-volatile; SOA is semi-volatile and also has multiphase chemistry sources.

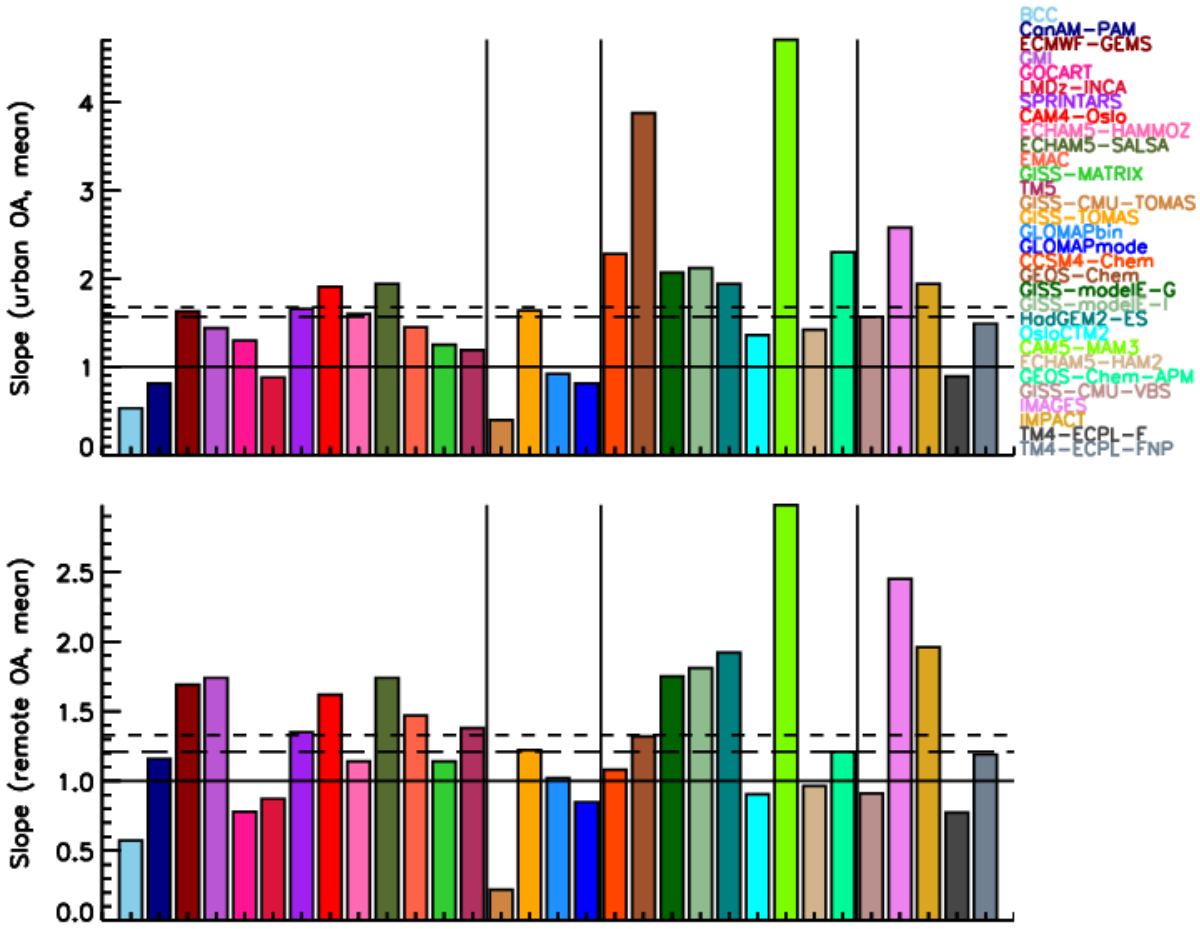

Fig. S 7. Same as Fig. S 6 for OA measurements.

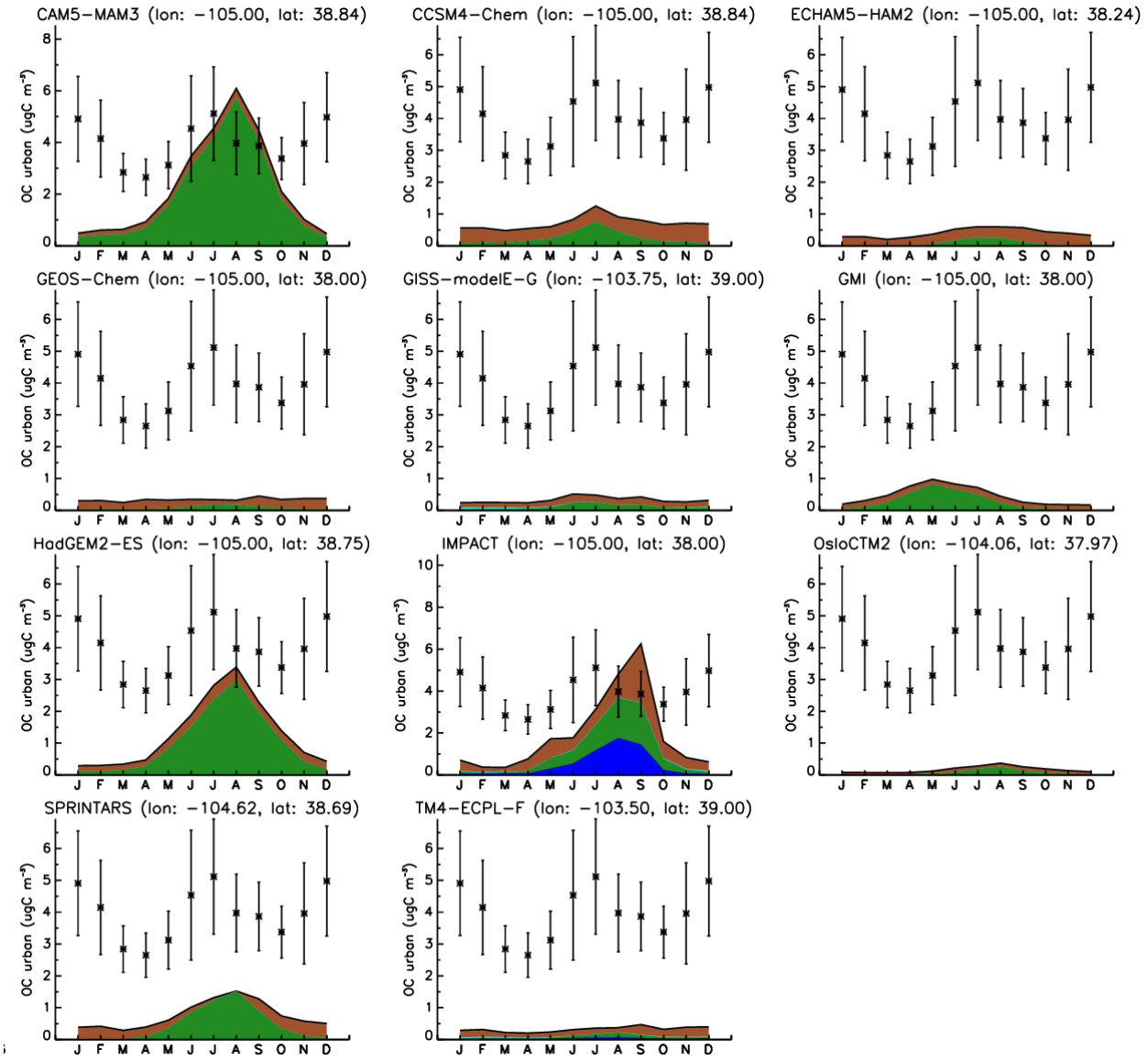

Fig. S 8. OC seasonal variability of OA chemical composition for the models not presented in the main paper, for Colorado, USA (urban). Colors are tPOC (brown), trSOC (green), ntrSOC (blue), mPOC (cyan), and MSA (orange). Each panel shows the model name and the coordinates of the center of the box where the station is located. Note the different scales on the y-axes.

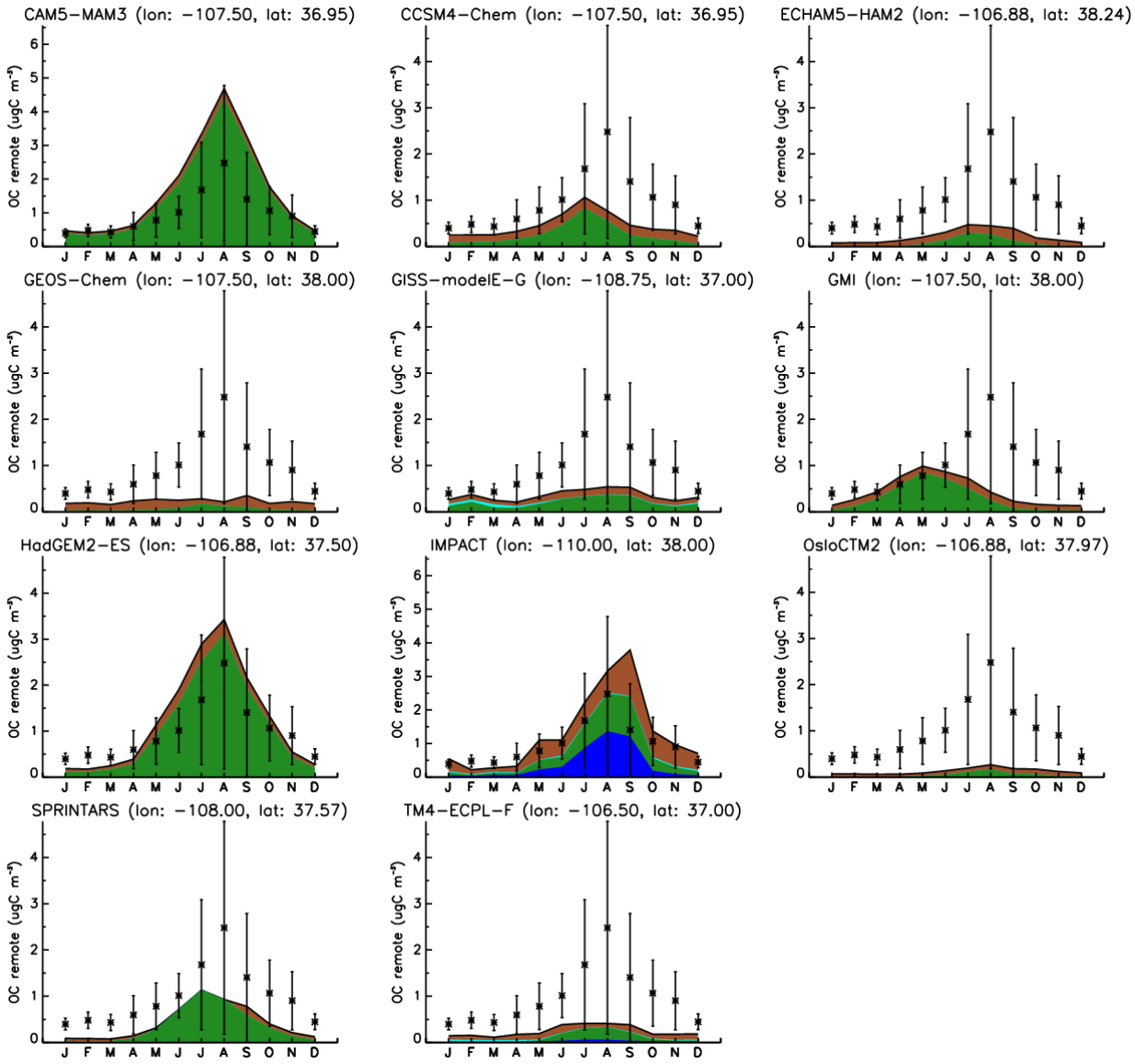

Fig. S 9. Same as Fig. S 8 for Colorado, USA (remote).

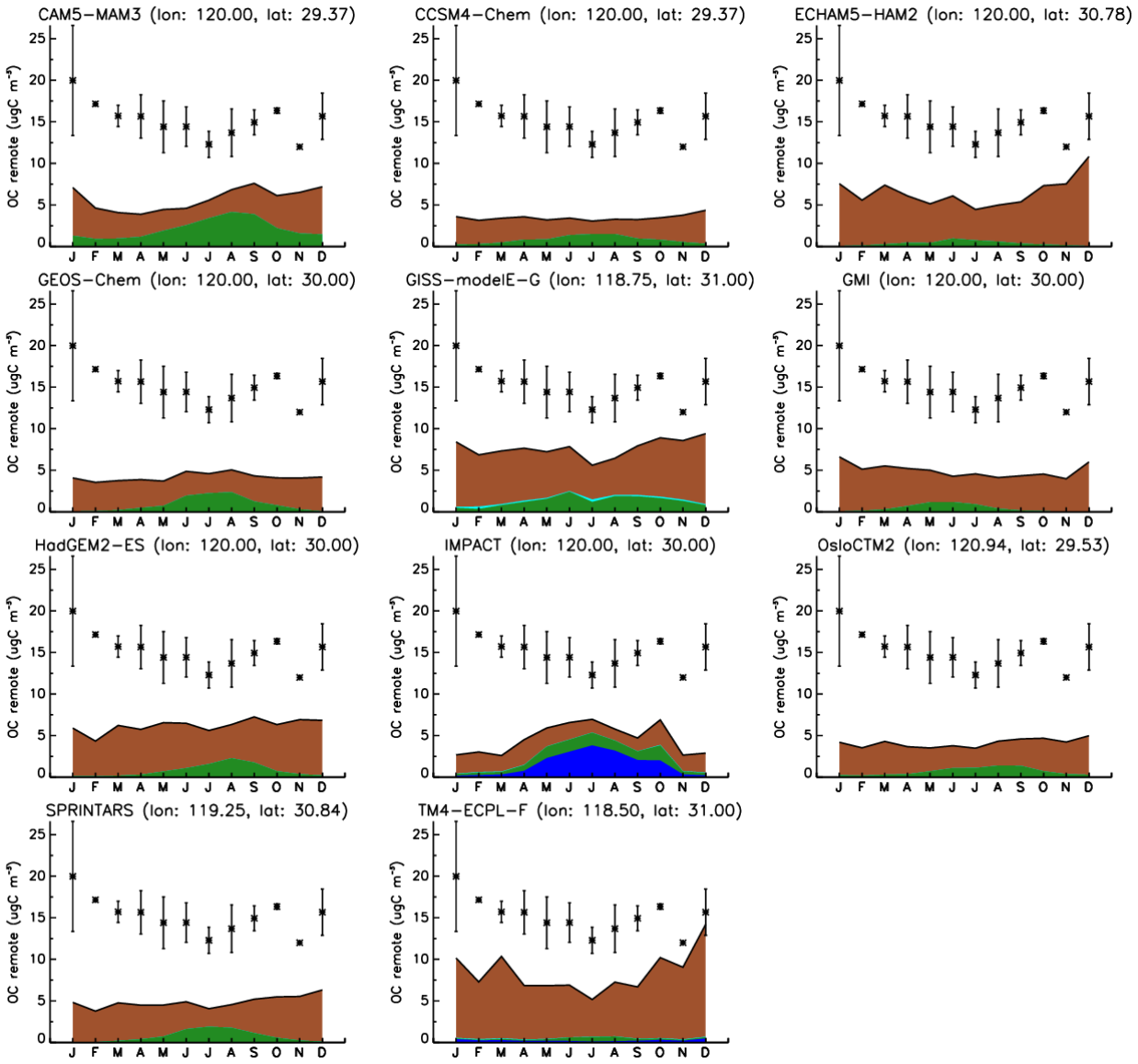

Fig. S 10. Same as Fig. S 8 for LinAn, China (remote).

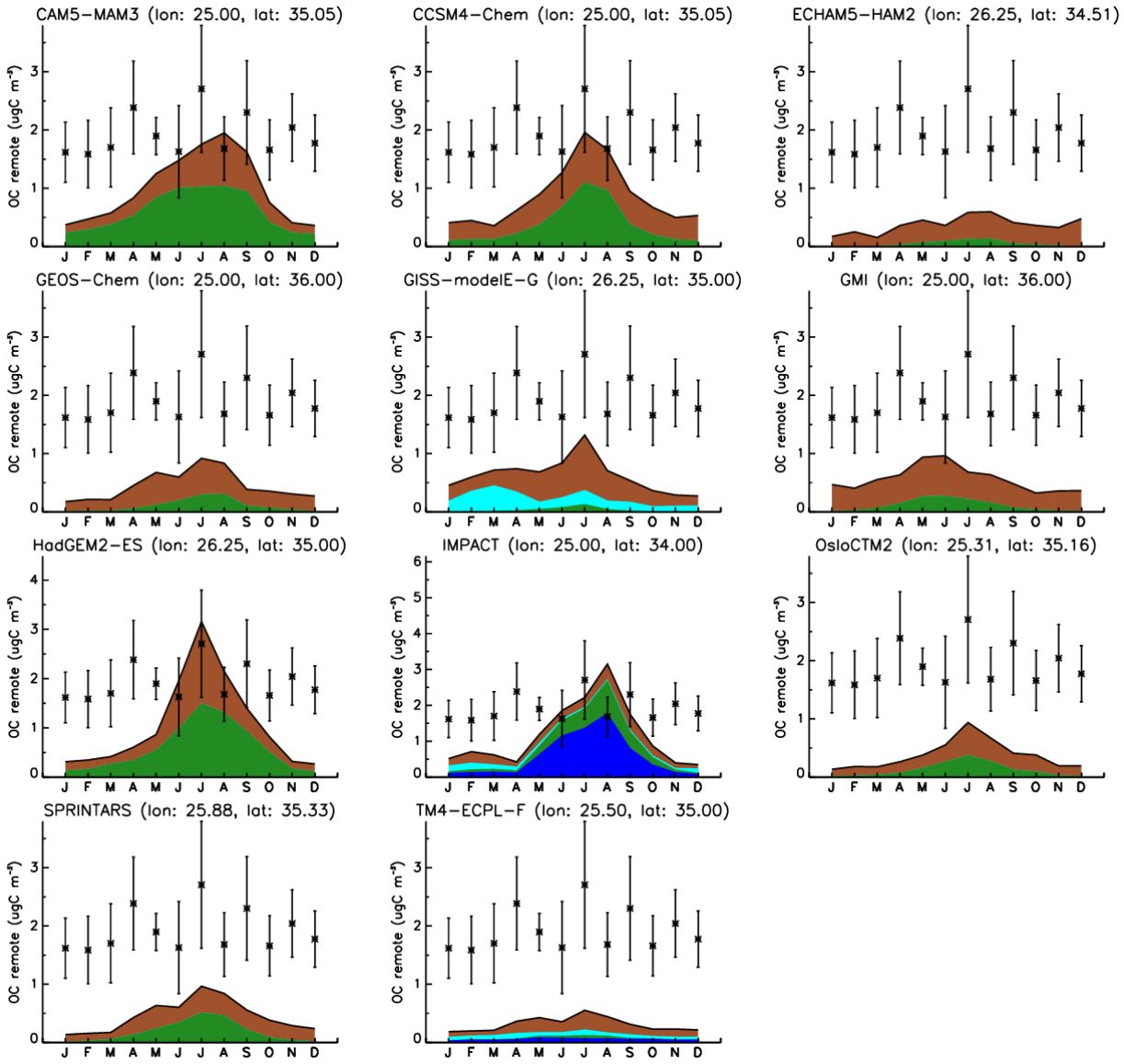

Fig. S 11. Same as Fig. S 8 for Finokalia, Greece (remote).

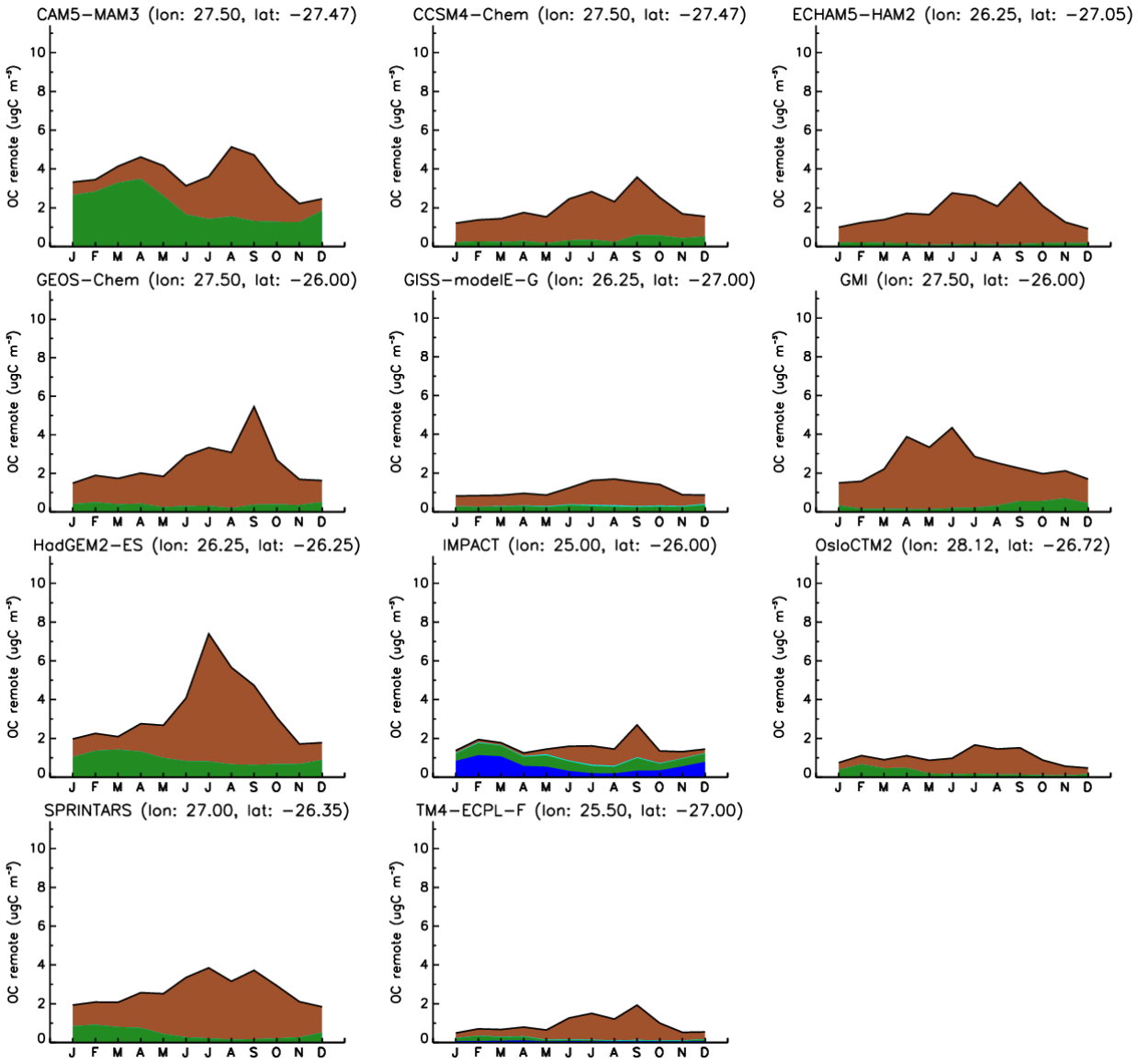

Fig. S 12. Same as Fig. S 8 at Welgegung, South Africa (remote). No measurements are plotted at the chemical composition panels, since measurements are OA and the chemical composition data from the models are OC.

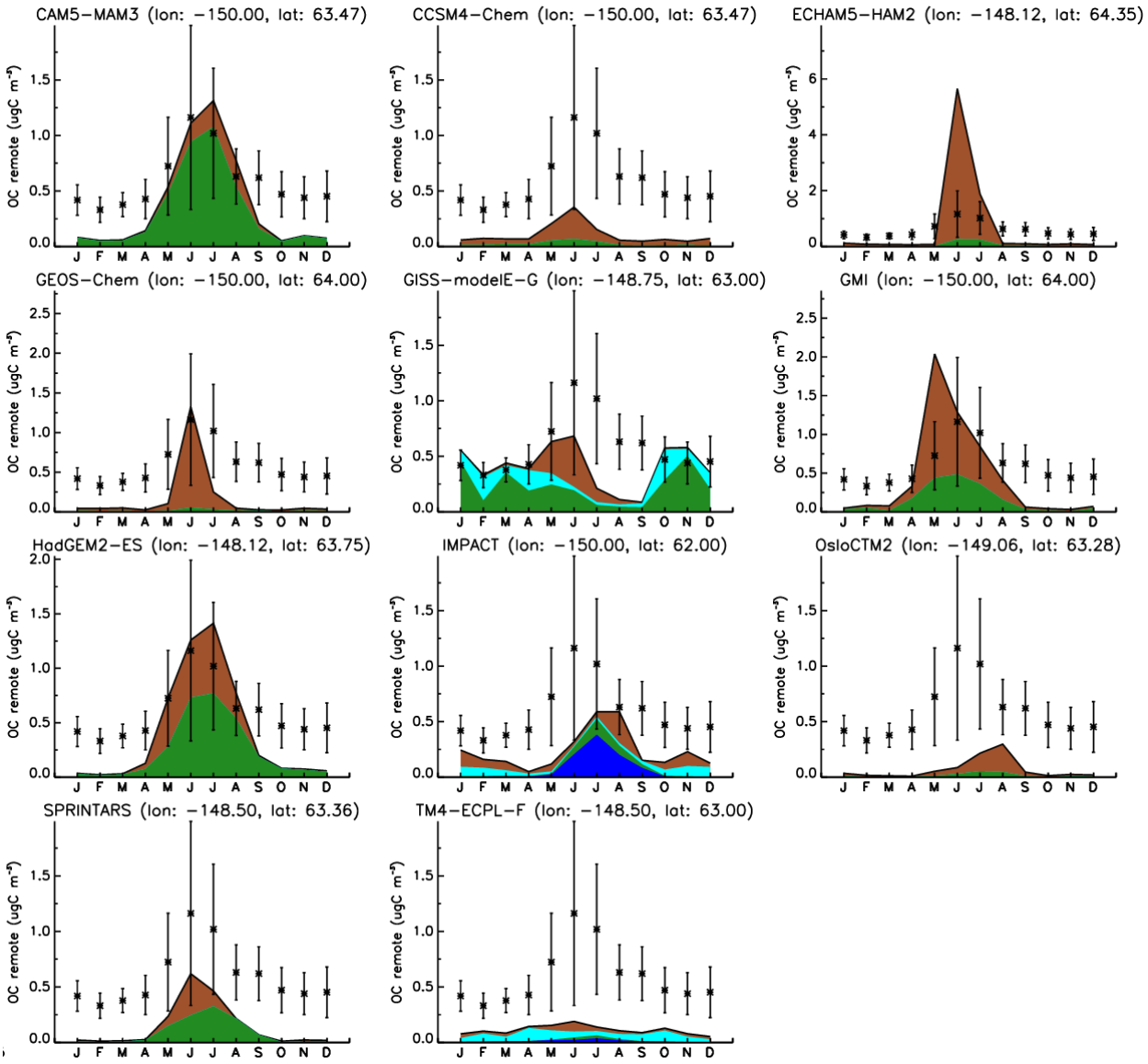

Fig. S 13. Same as Fig. S 8 for Alaska, USA (remote).

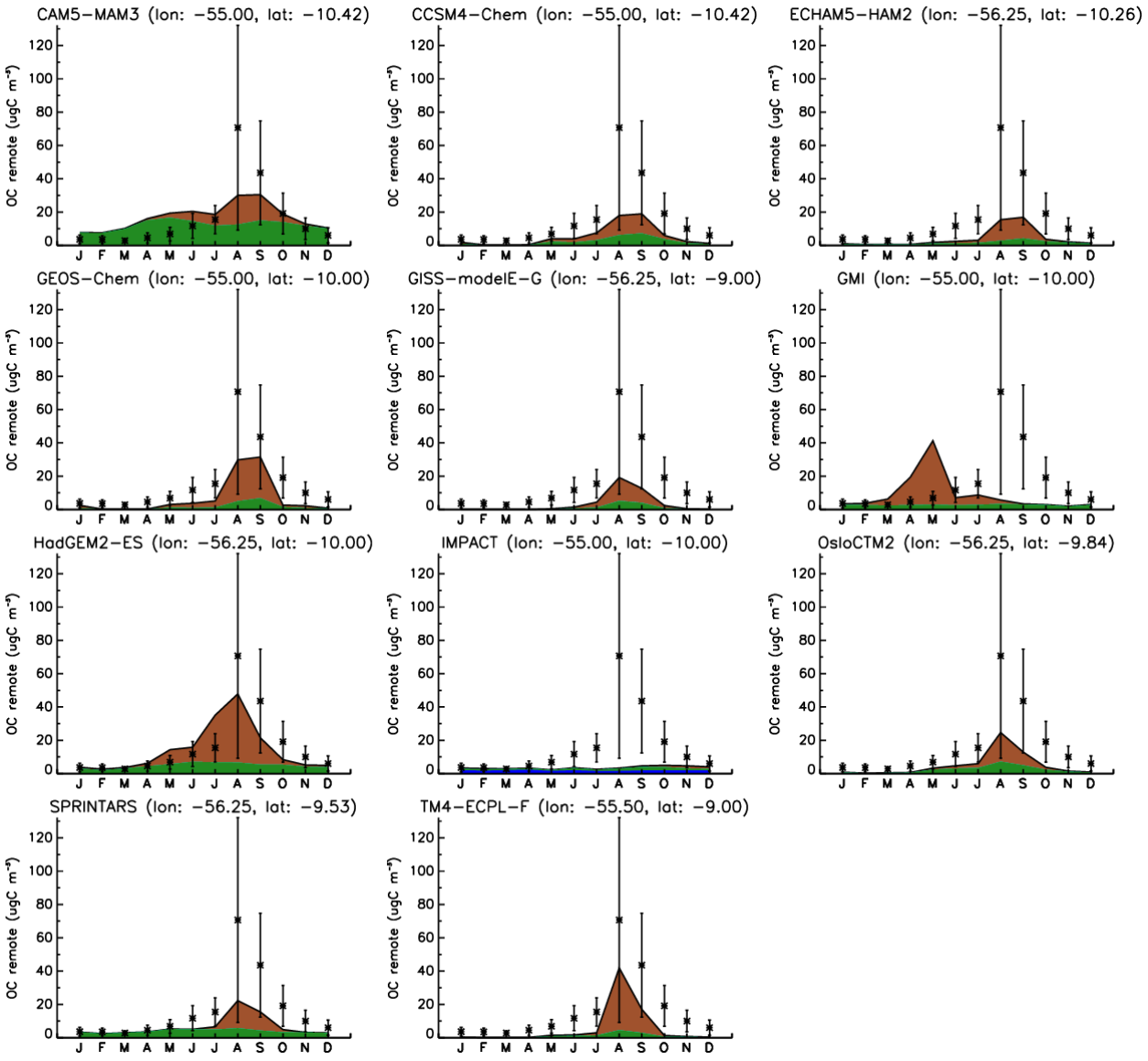

Fig. S 14. Same as Fig. S 8 for Alta Floresta, Brazil (remote).

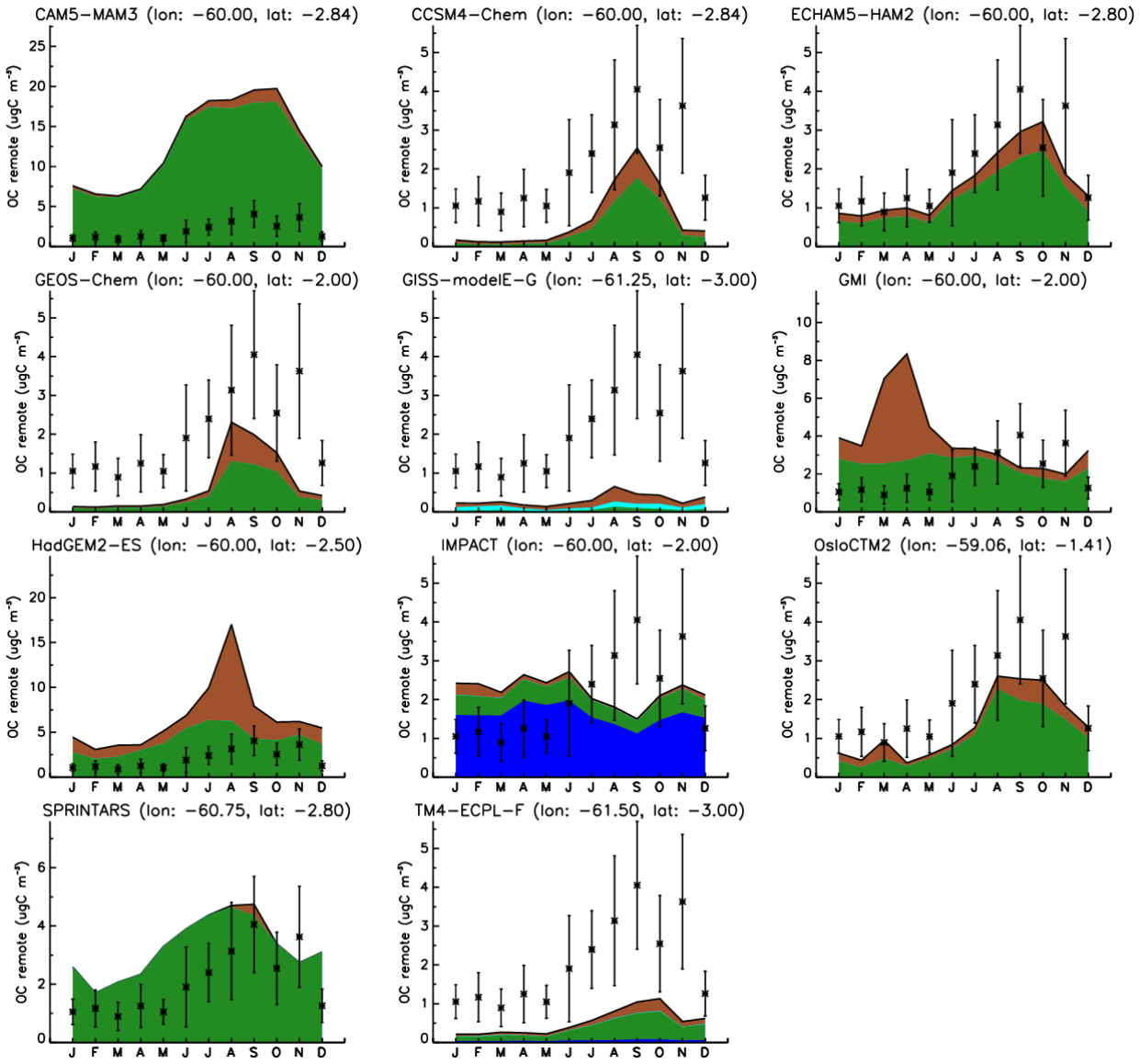

Fig. S 15. Same as Fig. S 8 for Manaus, Brazil (remote).

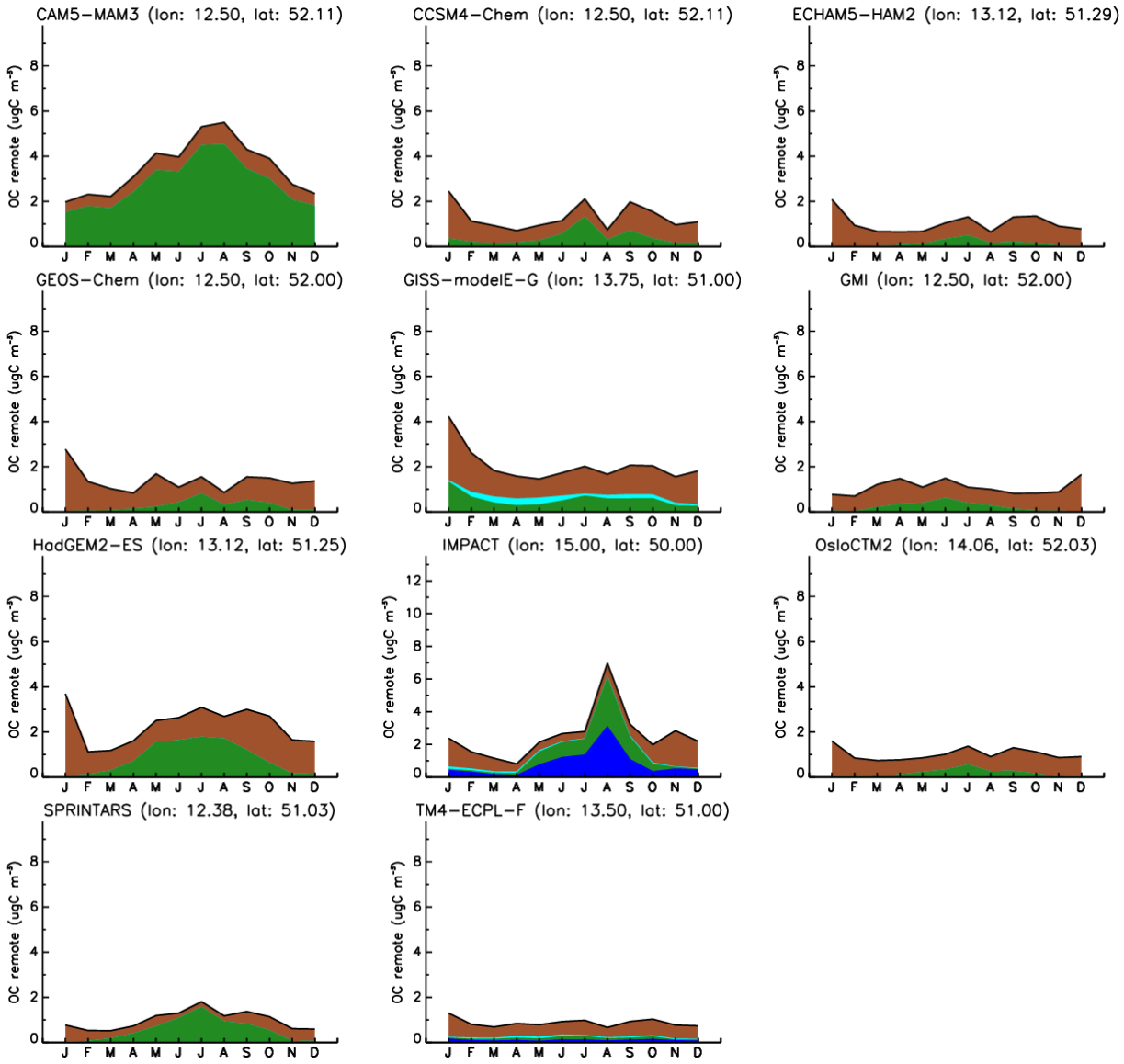

Fig. S 16. Same as Fig. S 12 for Melpitz, Germany (remote).

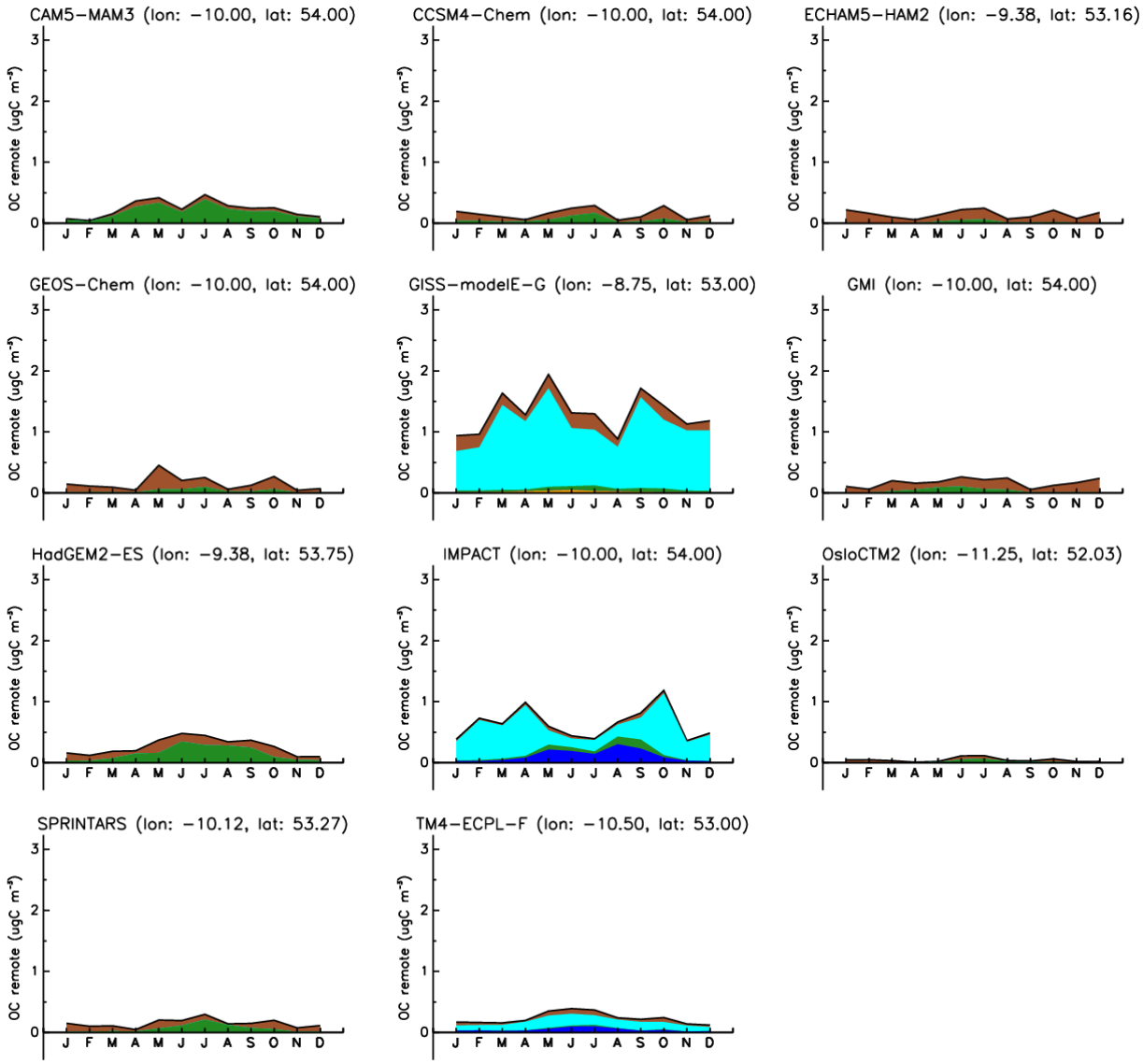

Fig. S 17. Same as Fig. S 12 for Mace Head, Ireland (remote).

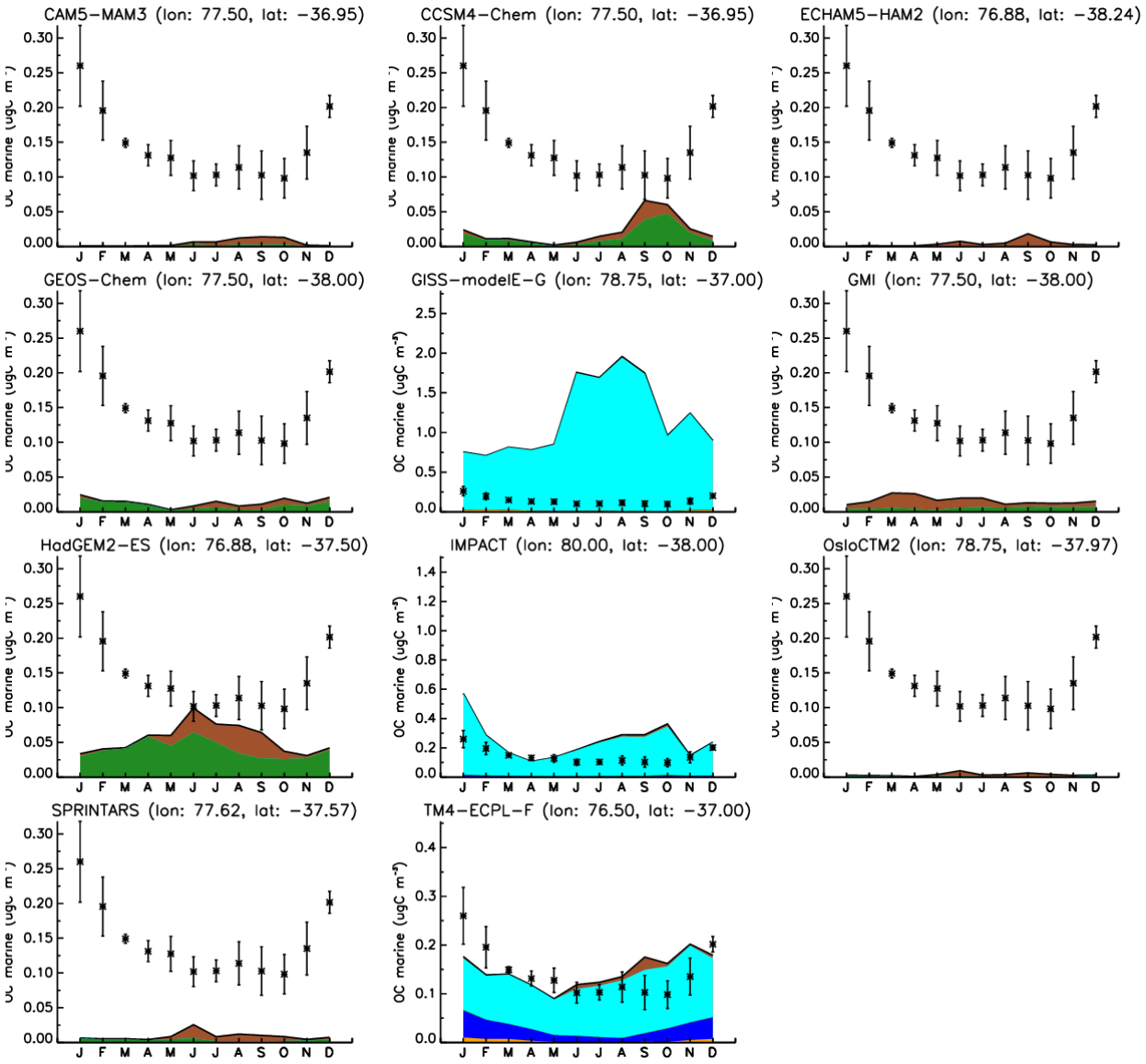

Fig. S 18. Same as Fig. S 8 for Amsterdam Island, Indian Ocean (marine).

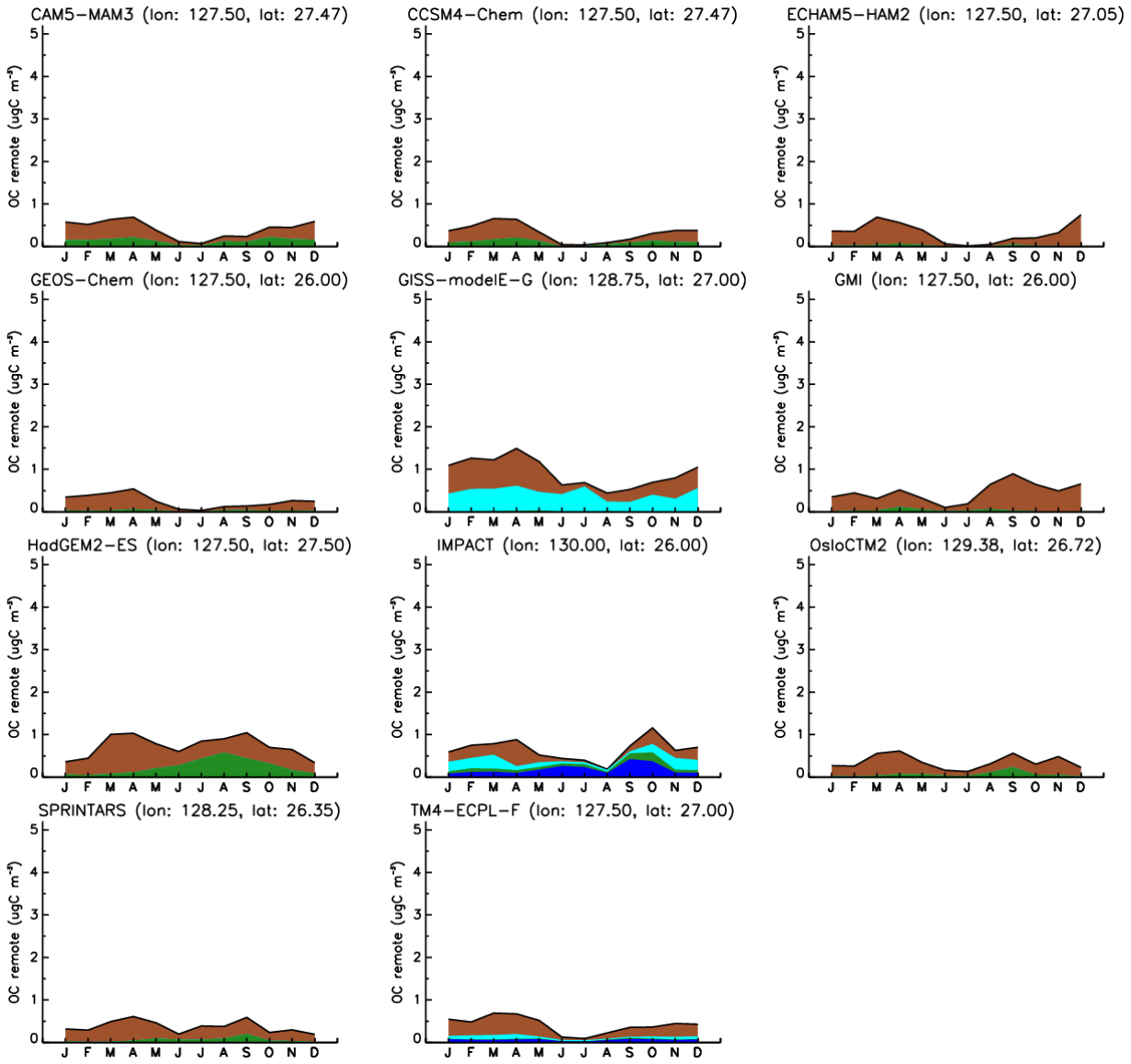

Fig. S 19. Same as Fig. S 12 for Okinawa, Japan (marine).

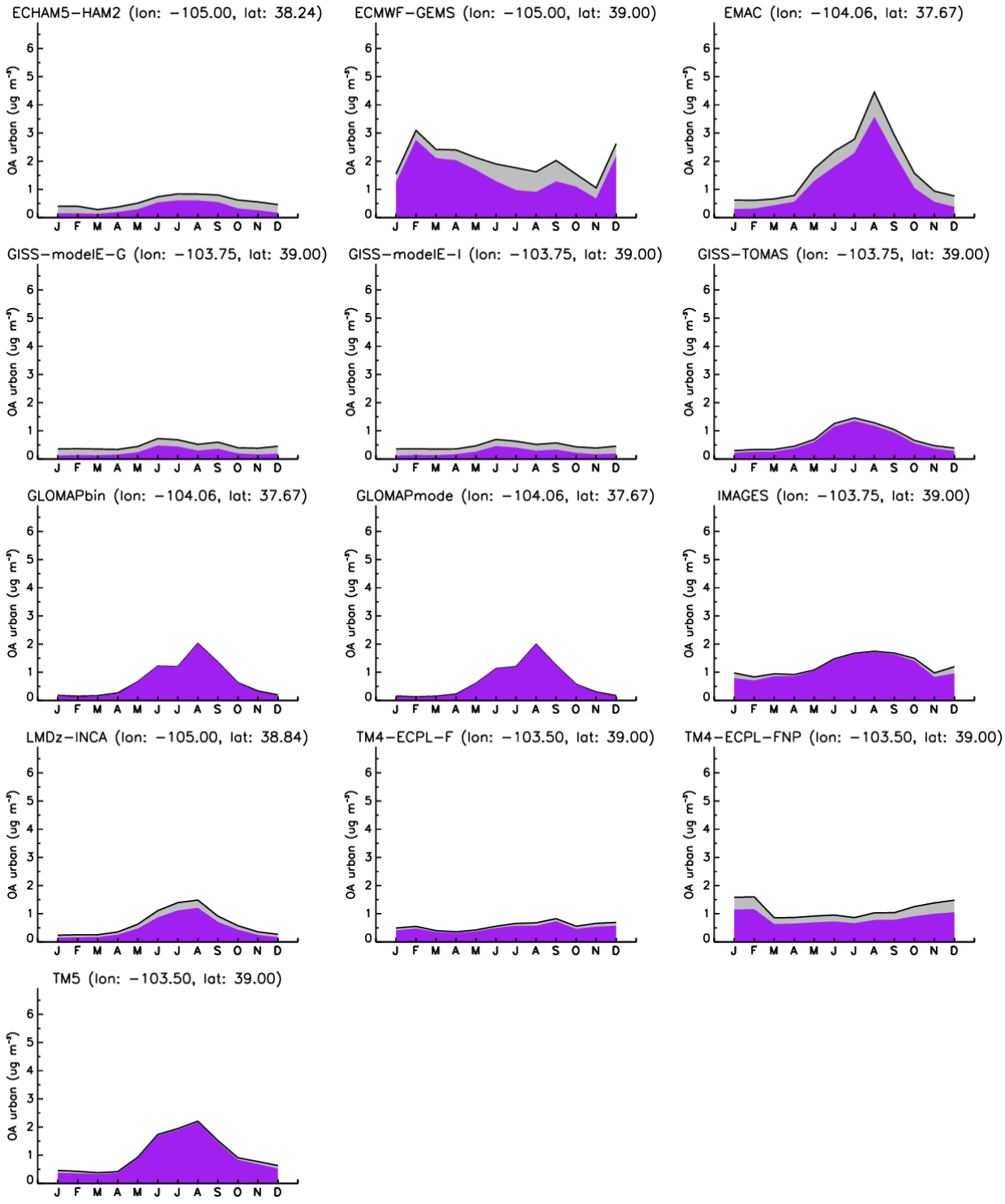

Fig. S 20. Same as Fig. S 8 for OA. The chemical composition (where available) is presented as measured by the AMS: HOA (grey) and OOA (purple).

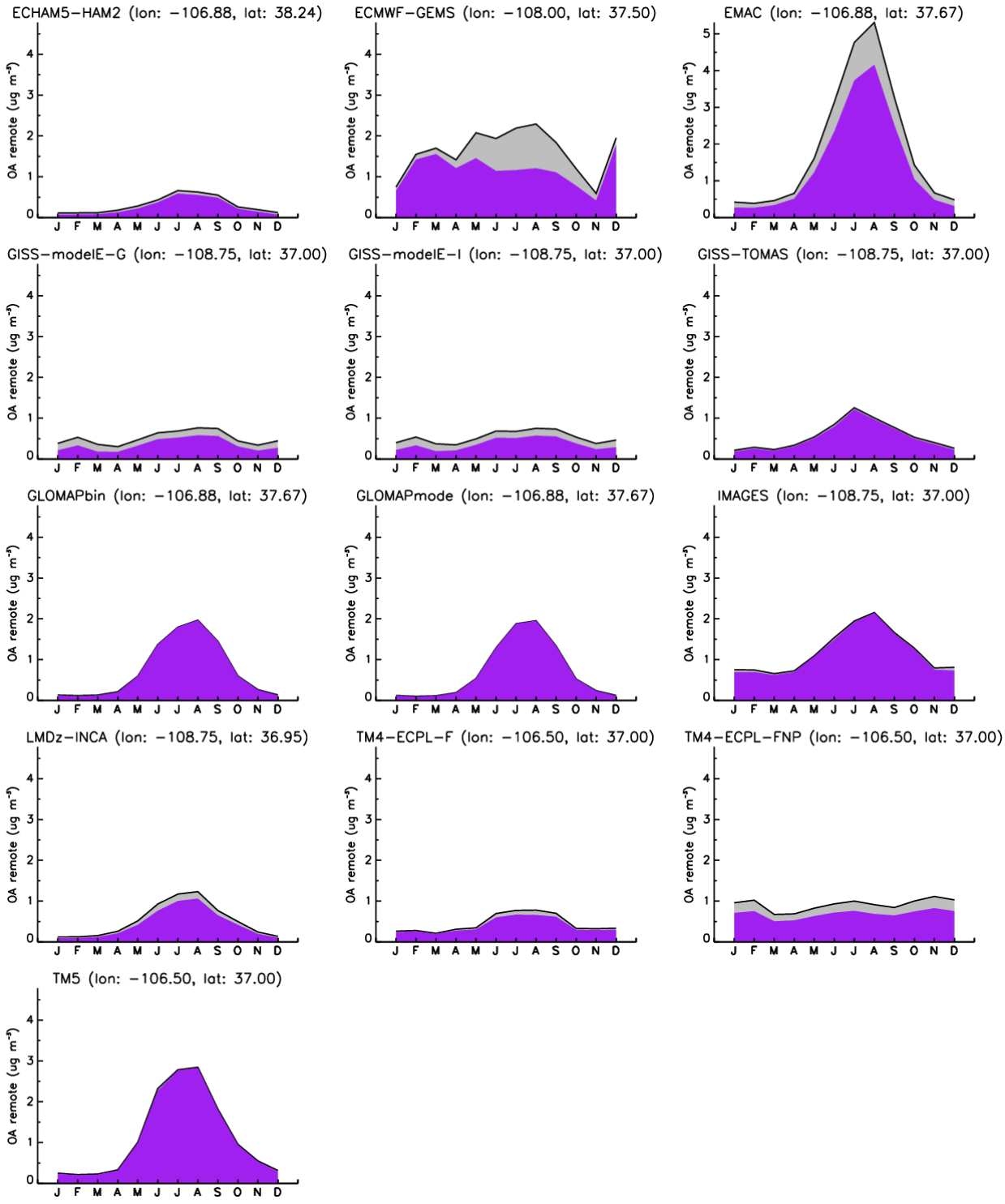

1

2 Fig. S 21. Same as Fig. S 20 for Colorado, USA (remote).

3

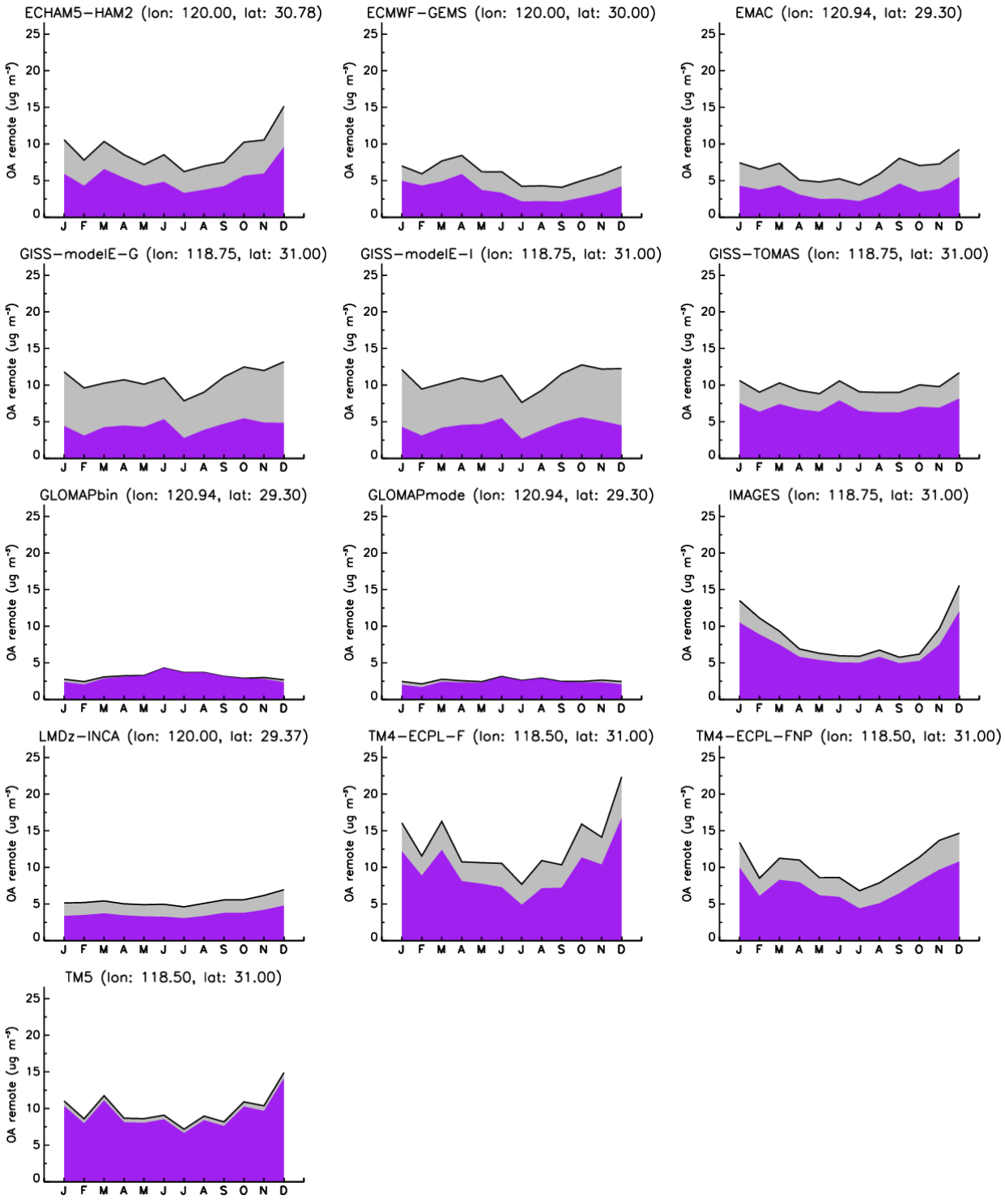

Fig. S 22. Same as Fig. S 20 for LinAn, China (remote).

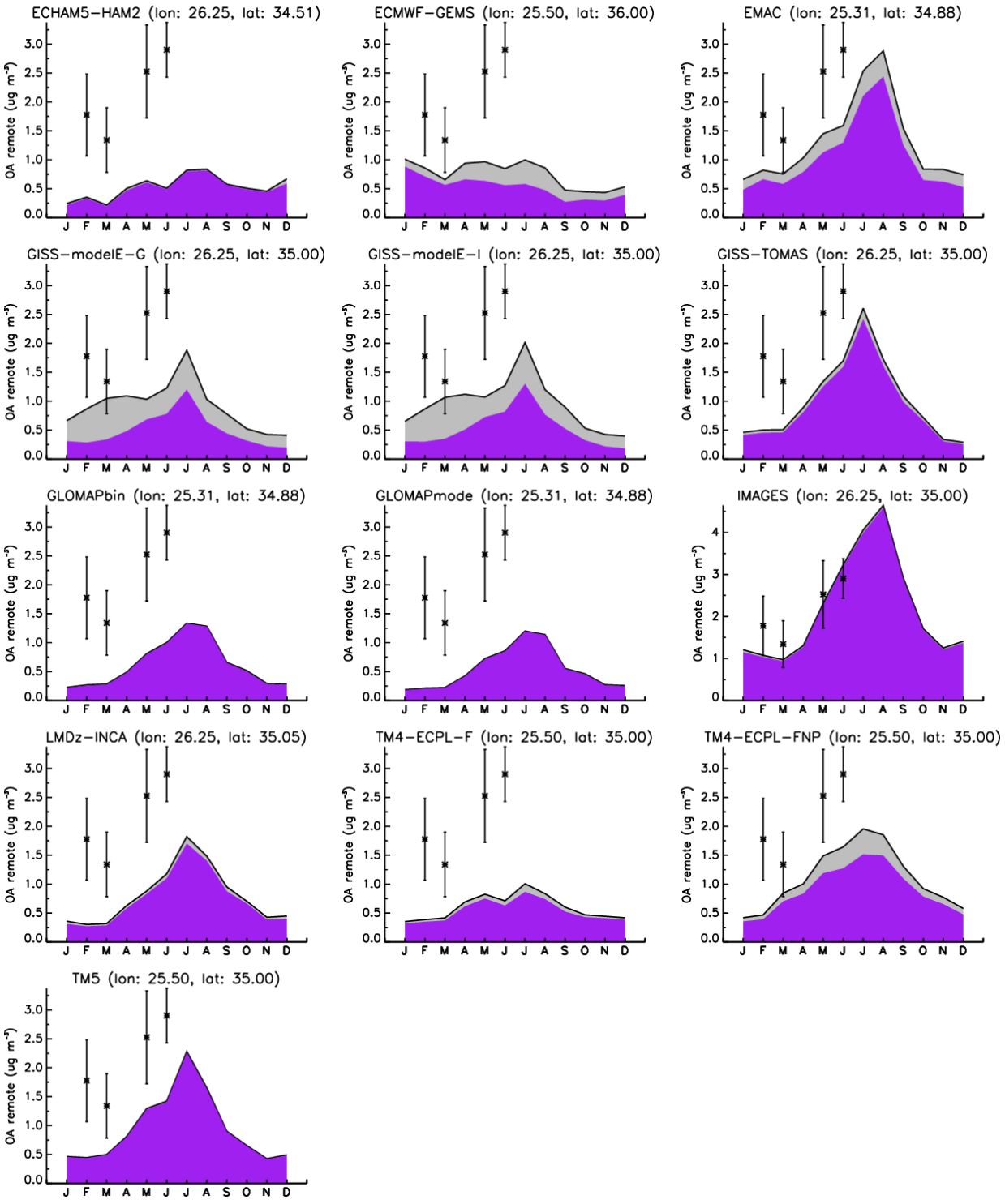

Fig. S 23. Same as Fig. S 20 for Finokalia, Greece (remote).

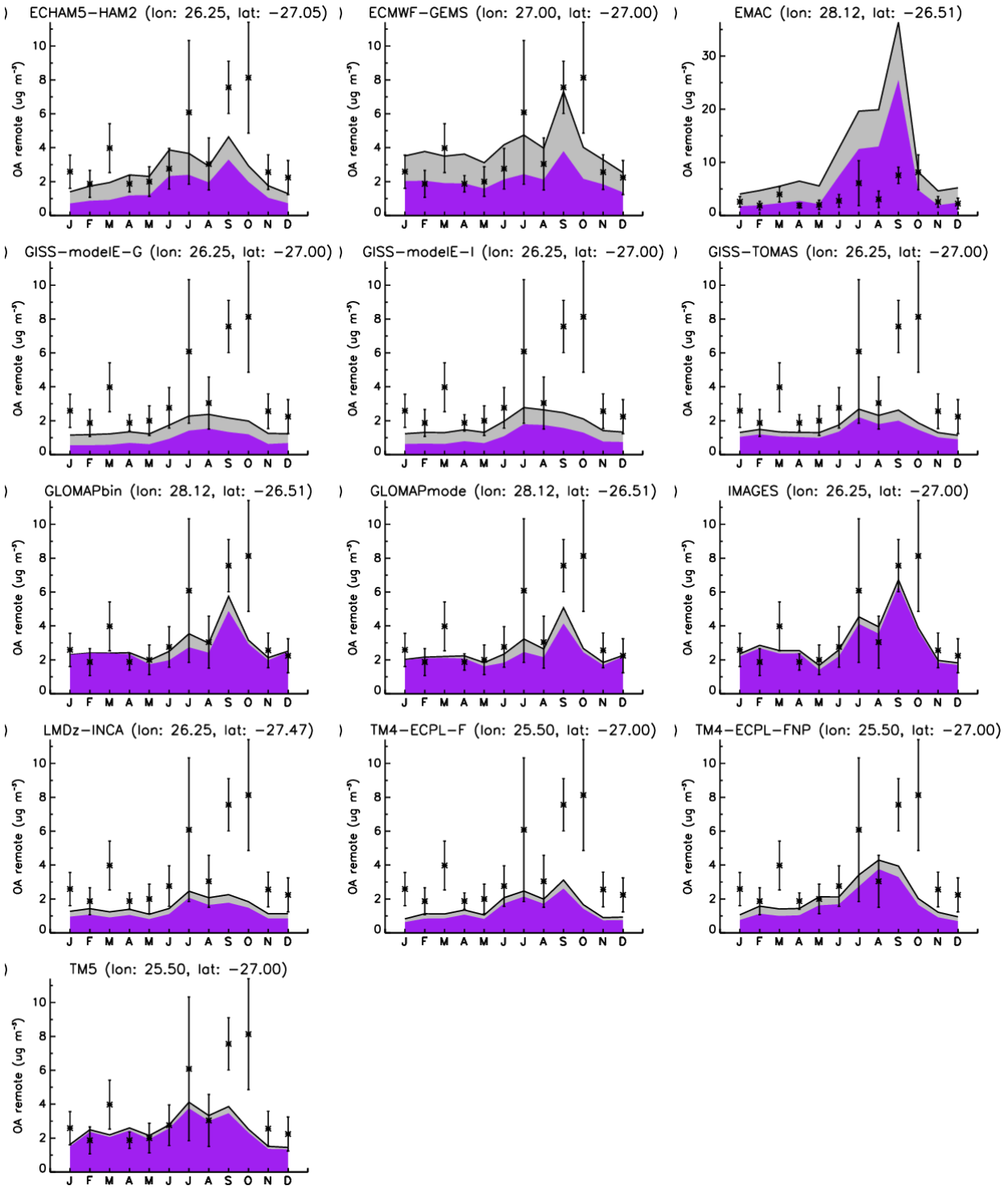

Fig. S 24. Same as Fig. S 20 for Welgegung, South Africa (remote).

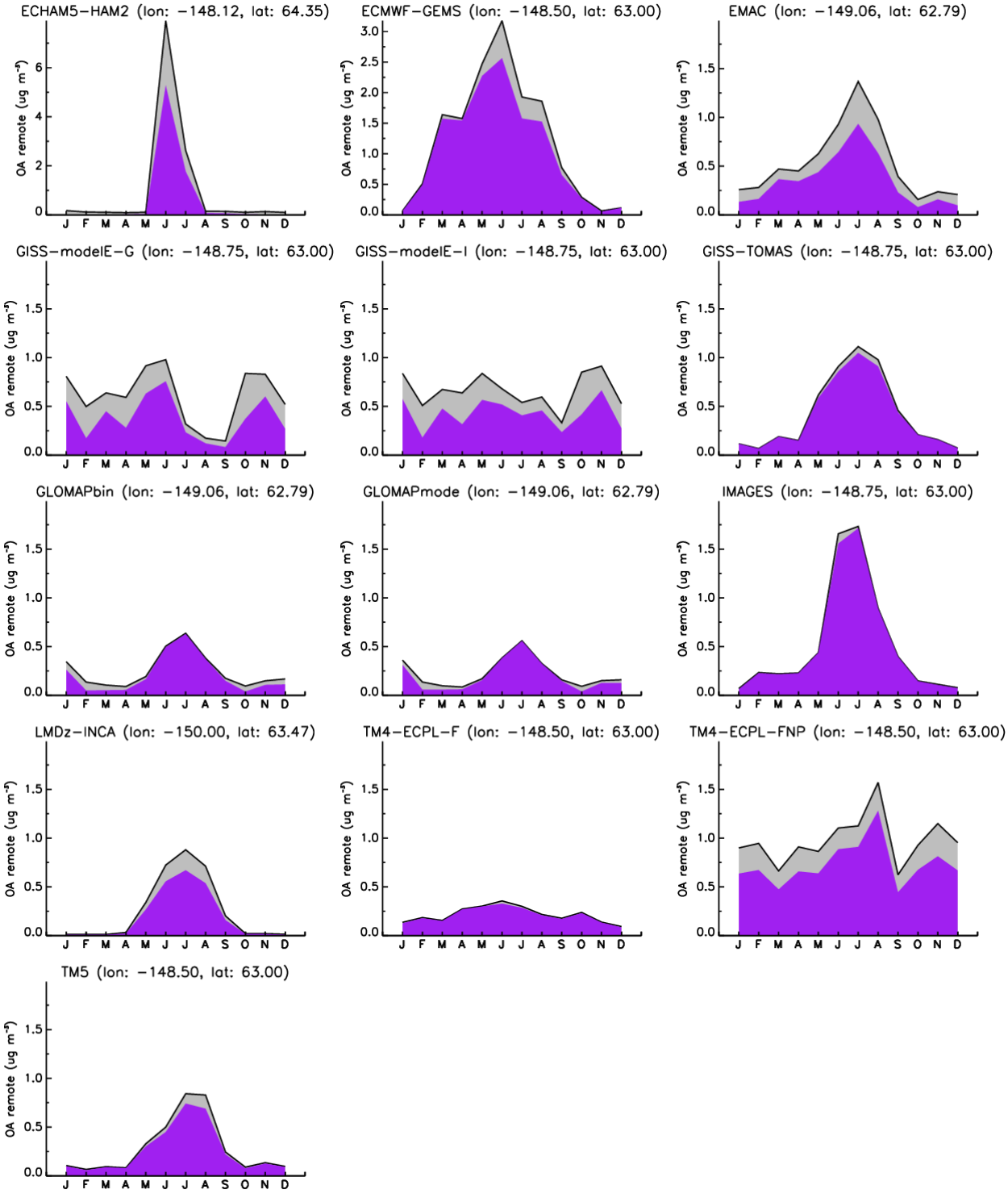

Fig. S 25. Same as Fig. S 20 for Alaska, USA (remote).

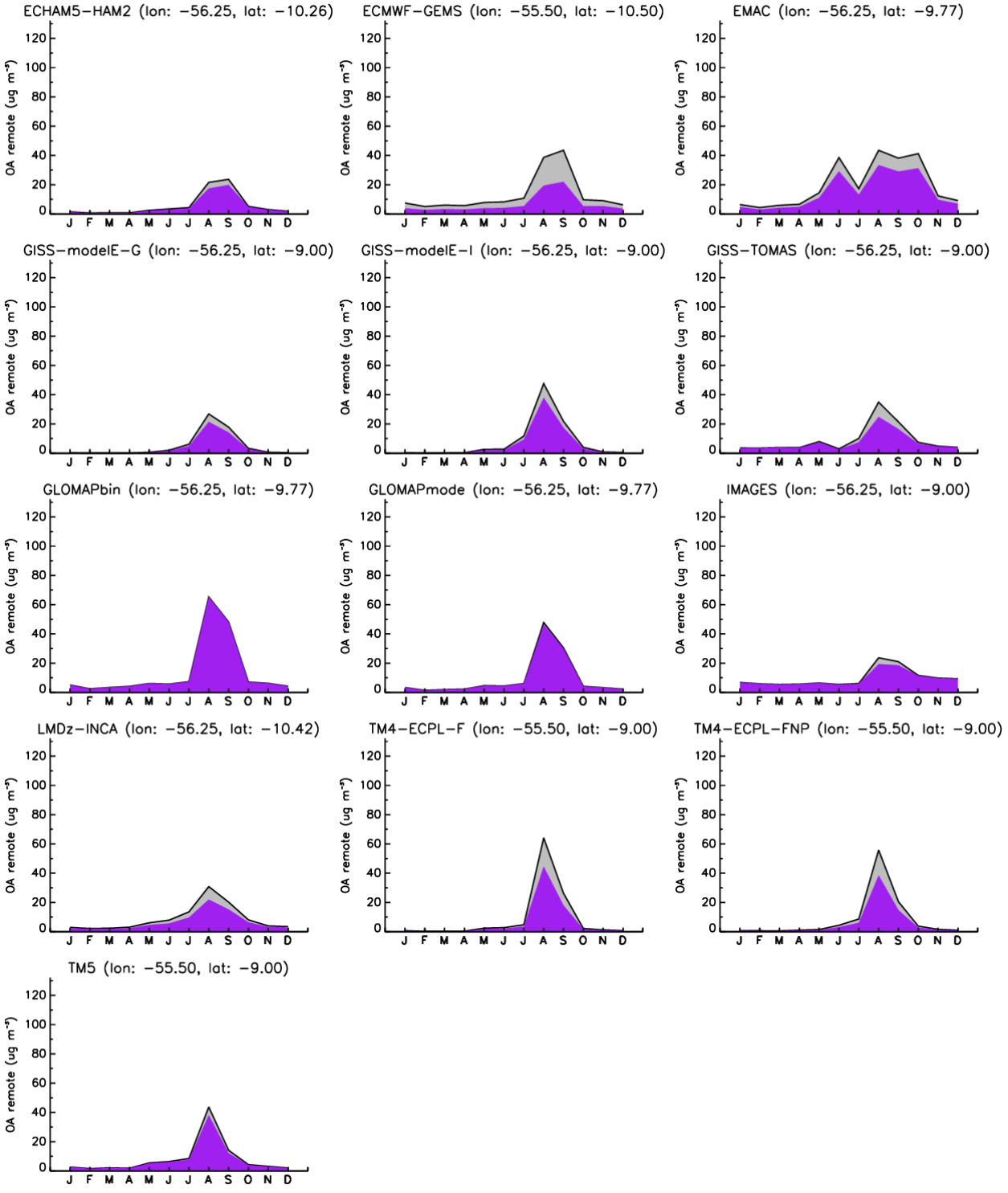

Fig. S 26. Same as Fig. S 20 for Alta Floresta, Brazil (remote).

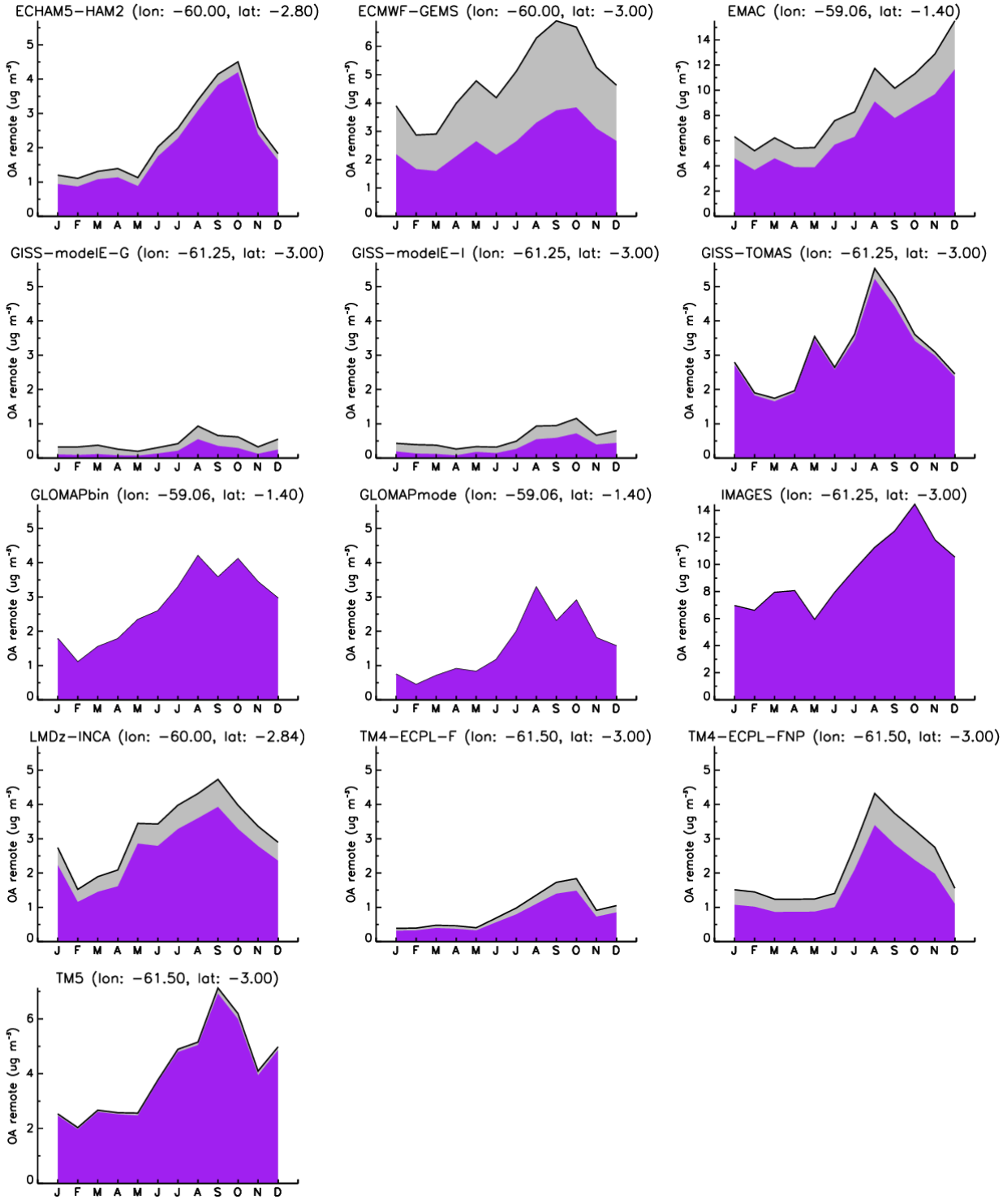

Fig. S 27. Same as Fig. S 20 for Manaus, Brazil (remote).

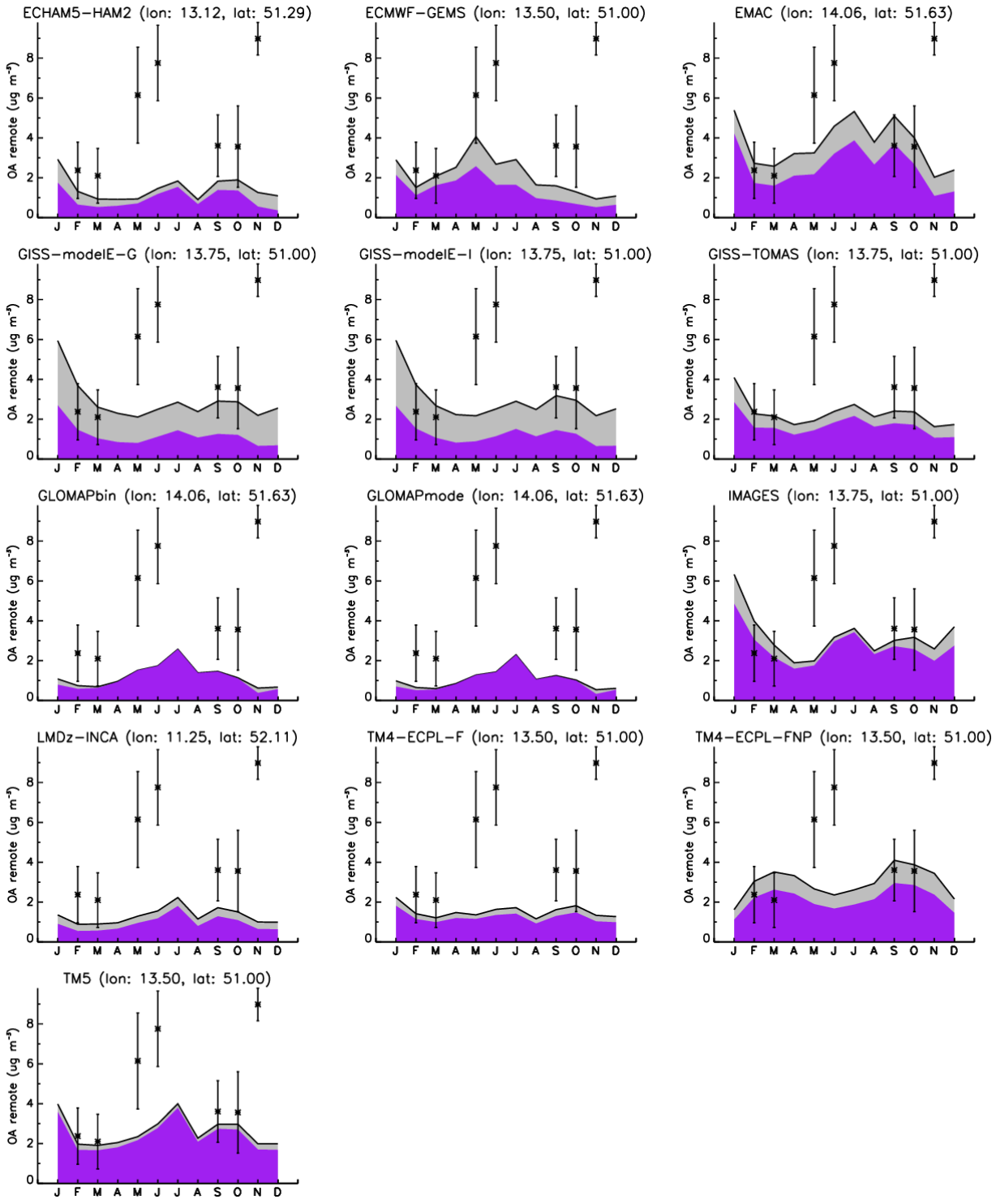

Fig. S 28. Same as Fig. S 20 for Melpitz, Germany (remote).

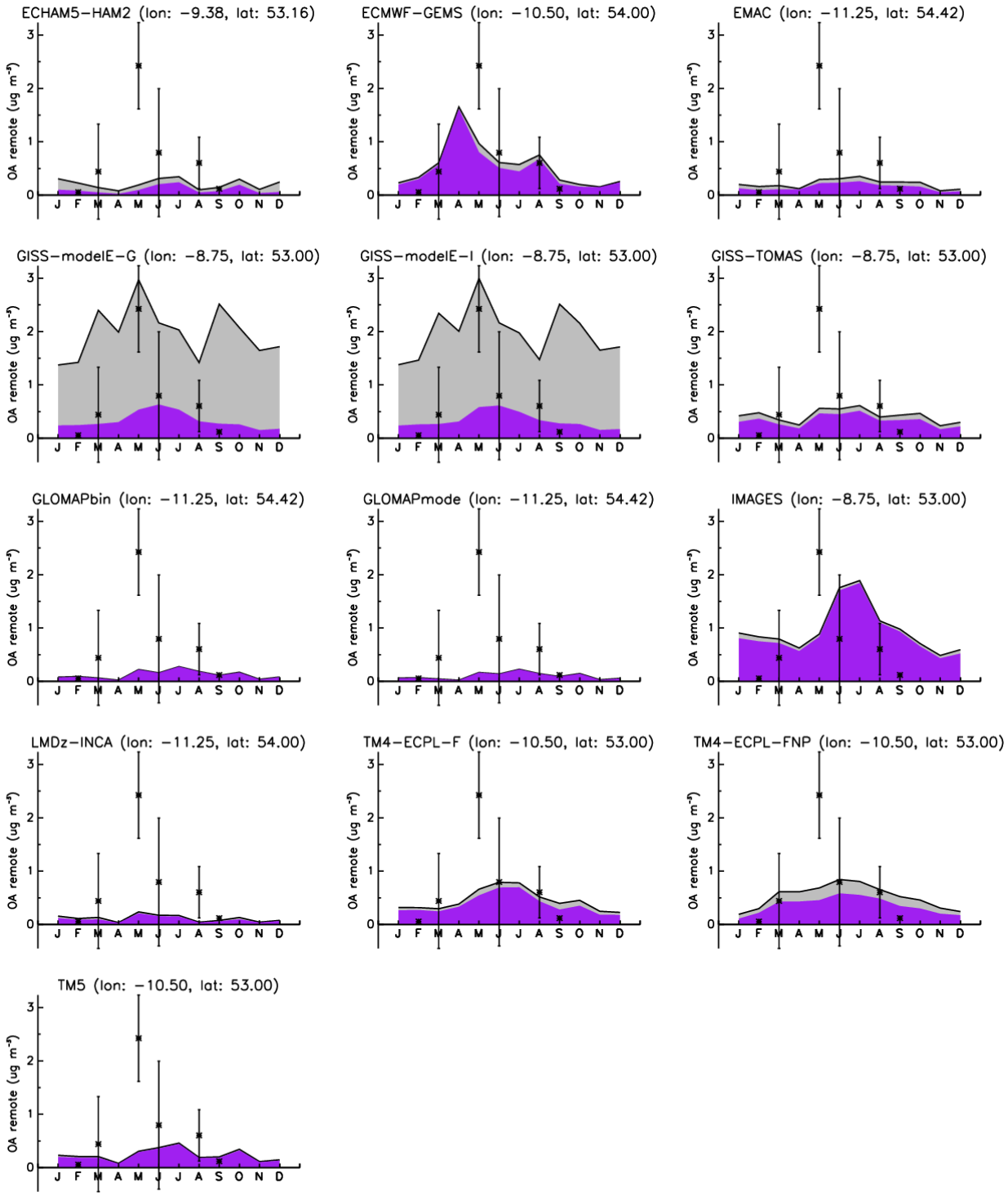

1

2 Fig. S 29. Same as Fig. S 20 for Mace Head, Ireland (remote).

3

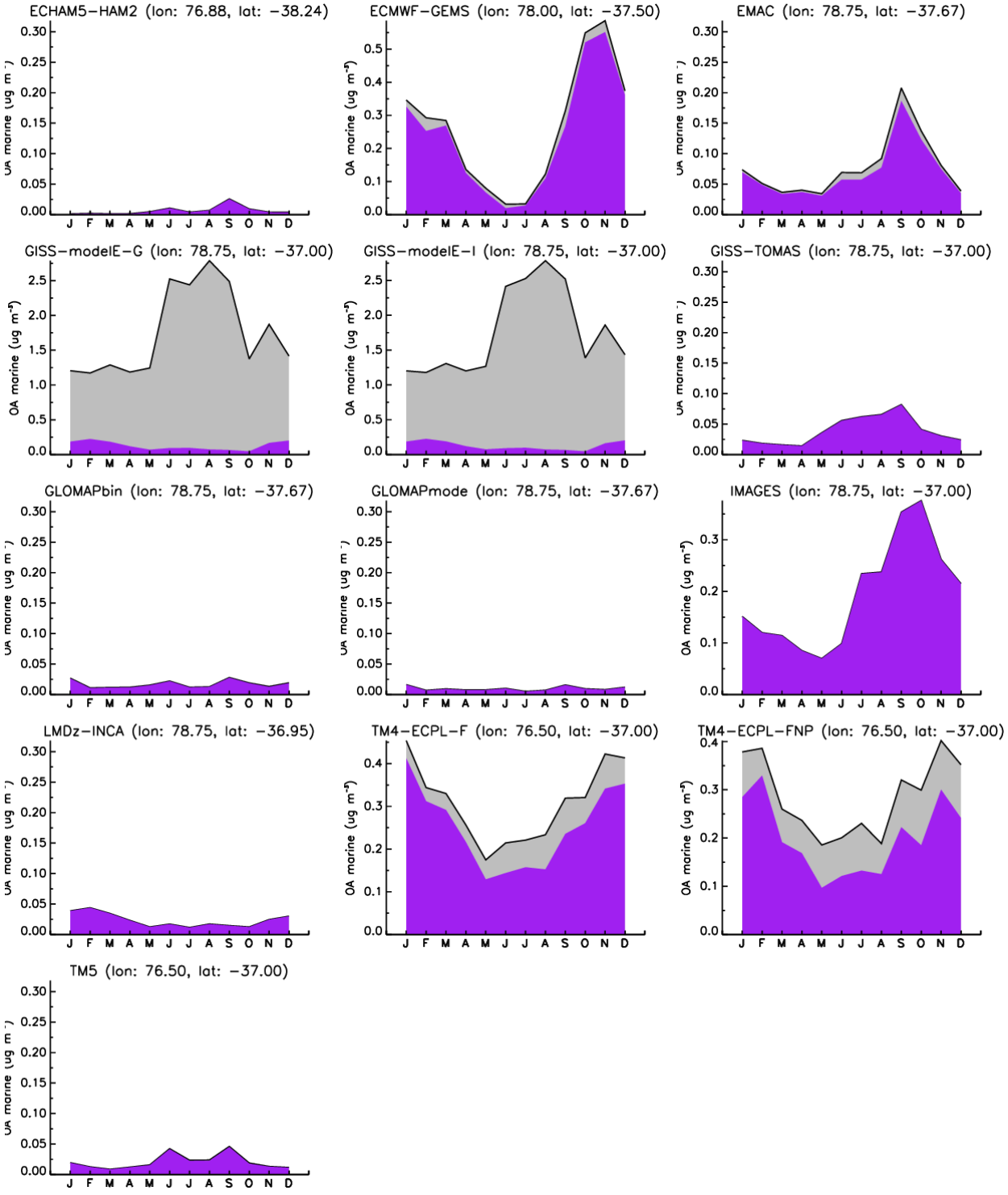

Fig. S 30. Same as Fig. S 20 for Amsterdam Island, Indian Ocean (marine).

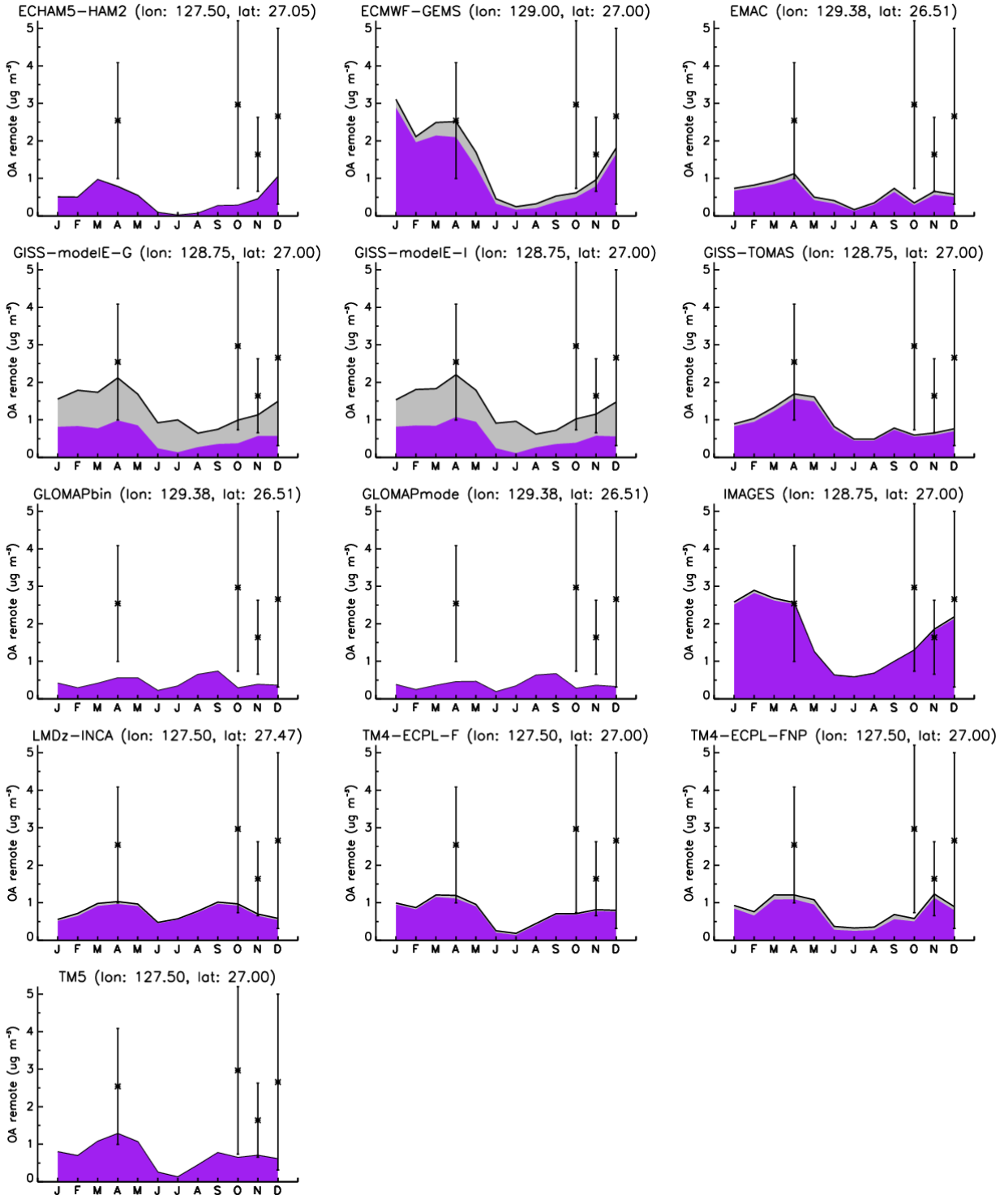

1

2 Fig. S 31. Same as Fig. S 20 for Okinawa, Japan (marine).